Open access • Journal Article • DOI:10.1029/2002JB002125

Cenozoic river profile development in the Upper Lachlan catchment (SE Australia) as a test of quantitative fluvial incision models — Source link

Pieter van Beek, Paul Bishop

Institutions: Joseph Fourier University, University of Glasgow

Published on: 01 Jun 2003 - Journal of Geophysical Research (John Wiley & Sons, Ltd)

Topics: Stream power and Fluvial

Cenozoic river profile development in the Upper Lachlan catchment (SE Australia) as a test of quantitative fluvial incision models.

Pieter van der Beek, Paul Bishop

Cenozoic river profile development in the Upper Lachlan catchment (SE Australia) as a test of quantitative fluvial incision models

Peter van der Beek[1] and Paul Bishop[2]

[1] *Laboratoire de Géodynamique des Chaînes Alpines, Université Joseph Fourier, 38041 Grenoble Cedex, France*

[2] *Department of Geography and Topographic Science, University of Glasgow, Glasgow G12 8QQ, U.K.*

Journal of Geophysical Research, vol. 108, 10.1029/2002JB002125, 2003.

ABSTRACT

We have used Early Miocene valley-filling basalts to reconstruct fluvial long profiles in the Upper Lachlan catchment, SE Australia, in order to use these as well-constrained initial conditions in a forward model of fluvial incision. Many different fluvial incision algorithms have been proposed and it is not clear at present which one of these best captures the behavior of bedrock rivers. We test five different formulations; the ability of these models to reproduce the observed present-day stream profiles and amounts of incision is assessed using a weighted-mean misfit criterion as well as the structure of the misfit function. The results show that for all models, parameter combinations can be found that reproduce the amounts of incision reasonably well. However, for some models, these best-fit parameter combinations do not seem to have a physical significance, whereas for some others, best-fit parameter combinations are such that the models tend to mimic the behavior of other models. Overall best-fit model predictions are obtained for a Detachment-Limited Stream Power model or an 'Undercapacity' model that includes a river width term that varies as a function of drainage area. The uncertainty in initial conditions does not have a strong impact on model outcomes. The model results suggest, however, that lithological variation may be responsible for variations in parameter values of a factor of three to five.

1. INTRODUCTION

The processes of fluvial erosion and transport constitute the main controls on continental morphology and sediment fluxes [e.g., *Hay*, 1998; *Hovius*, 2000]. They also form a prime ingredient of numerical landscape evolution models, which have become instrumental in exploring tectonic, climatic and erosional controls on the development of continental relief [*Beaumont et al.*, 2000; *Willett*, 1999]. A quantitative understanding of these processes is therefore essential to comprehend the interaction between tectonics and long-term landscape development, as well as global sediment fluxes. Whereas fluvial transport in alluvial systems has long been the focus of quantitative study [e.g., *Leopold et al.*, 1964], processes in bedrock rivers have only recently been studied in some detail, and an adequate general theory for incision and sediment transport by bedrock rivers is yet to be formulated [cf. *Tinkler and Wohl*, 1998; *Tucker and Whipple*, 2002].

The majority of workers agree that the rate of bedrock incision by a river should be controlled in some way by fluvial stream power, that is, should be a function of the river's local slope and discharge [*Howard et al.*, 1994; *Whipple and Tucker*, 1999]. The functional

form of the relationship, however, as well as the physical processes involved, remains controversial. Whereas a linear relationship between fluvial stream power per unit width and carrying capacity appears well established [*Leopold et al.*, 1964; *Willgoose et al.*, 1991], the relationship between stream power and the rate of bedrock incision may be highly nonlinear [*Howard et al.*, 1994; *Whipple et al.*, 2000a]. In many cases, it is not clear whether incision rates are limited by the processes of bedrock detachment themselves, or by the ability of the river to transport the sediments supplied by incision and flushed into it from neighboring hill-slopes. Models of river incision have been proposed that more explicitly take into account the role of fluvial sediment load [*Beaumont* et al, 1992; *Sklar and Dietrich*, 1998] or the influence of thresholds [*Bagnold,* 1977; *Howard*, 1994] on river incision.

In order to discriminate between the various models of bedrock incision by rivers, one can either attempt to study in detail the physical processes leading to bedrock incision [e.g., *Hancock et al.*, 1998; *Whipple et al.*, 2000a], map present-day sediment flux and erosion rates in river channels [e.g., *Hartshorn et al.*, 2002], or attempt to distil useful information from fluvial long profile forms. Data that are relevant to the former two approaches are extremely scarce. Most studies that have used river long profiles to test bedrock incision models have assumed that incision of the rivers studied was in dynamic equilibrium with local rock uplift rates, so that the form of the fluvial profile is constant over time [e.g., *Slingerland et al.*, 1998; *Snyder et al.*, 2000]. However, whereas equilibrium long profiles may provide constraints on the parameter values for any particular model, they appear relatively undiagnostic in discriminating between different models [*Slingerland et al.*, 1998; *Tucker and Whipple*, 2002; *Whipple and Tucker*, 2002]. Moreover, except in the specific conditions of sustained high rock uplift and incision rates, rivers will generally not be in dynamic equilibrium and their forms will change over time. Studying the development of fluvial form over time after some initial disturbance may lead to significant progress in our understanding of the dynamics of, and controls on, bedrock river incision [e.g., *Howard et al.,* 1994; *Stock and Montgomery*, 1999]. However, a precise control on initial conditions and timing is crucial in such studies and only a few locations where such control may be achieved have been recognized. Although remnants of paleo-river profiles (in the form of abandoned fluvial terraces or paleovalleys) abound, the correlation and precise dating of these remnants often pose severe difficulties.

The Upper Lachlan River and its tributaries in southeastern (SE) Australia provide an excellent opportunity to study river long-profile development over temporal and spatial scales that are relevant to landscape-evolution models, and have been used previously to constrain parameter vealues entering into fluvial bedrock incision laws [*Stock and Montgomery*, 1999].

In the Upper Lachlan catchment, widespread remnants of basalt flows, which have been mapped in detail and precisely dated [*Bishop and Goldrick*, 2000; *Bishop et al.*, 1985; *Goldrick*, 1999; *Wellman and McDougall*, 1974], preserve Early Miocene river profiles that may serve as well-constrained initial conditions to test fluvial incision models. Moreover, the catchments bedrock lithology is relatively simple, its base-level history can be reconstructed with reasonable confidence, its Cenozoic climate history is well known and relatively stable, and it was not glaciated during the Quaternary. We have reconstructed the Early Miocene river profiles of the Lachlan River and three of its tributaries, and use these as the starting condition to run forward models of fluvial incision. The predicted present-day fluvial profiles and amounts of incision are quantitatively compared to the observed fluvial profiles and incision in order to test the capability of the different incision algorithms to simulate fluvial long profile development in this region.

In the following, we first briefly review the most widely used fluvial incision algorithms and their theoretical background. We then introduce the study area and present our data on paleo-river profiles and fluvial incision. Subsequently, we outline our modeling approach and present modeling results for different fluvial incision algorithms. Finally, we discuss our findings in the light of how these may aid in the selection of fluvial incision algorithms for numerical landscape evolution models, and what are the most important controls on river incision in our study area.

2. FLUVIAL INCISION MODELS

The most widely used formulation for fluvial incision is based on the hypothesis that incision rate should be proportional to either stream power (Ω), unit stream power (ω), or basal shear stress (τ) [*Bagnold*, 1977; *Howard et al.*, 1994]. The rate of fluvial incision $\dot{e}$ for all three of the above models may be cast in terms of the well-known 'Stream Power law' [*Bagnold,* 1977; *Howard et al.*, 1994; *Whipple and Tucker*, 1999]:

$$\dot{e} = K A^m S^n \tag{1}$$

where K is a dimensional constant [$L^{(1-2m)}$ T^{-1}], A is area [L^2], S is local stream gradient, and m and n are dimensionless exponents that depend on the specific physical model at the basis of (1): if $\dot{e} \propto \Omega$, then $m = n = 1$ [*Seidl and Dietrich,* 1992; *Seidl et al.*, 1994]; if $\dot{e} \propto \omega$, then $m \approx 0.5$ and $n = 1$; if $\dot{e} \propto \tau$, then $m \approx 0.3$ and $n \approx 0.7$ [*Howard et al.*, 1994; *Whipple and Tucker*, 1999]. The Stream Power incision law has been widely used to numerically model landscape

development [e.g., *Anderson*, 1994; *Tucker and Slingerland*, 1994; *Willett*, 1999] as well as to infer rock uplift rates directly from fluvial profile forms [*Finlayson et al.*, 2002; *Kirby and Whipple*, 2001; *Snyder et al.*, 2000].

An implicit assumption in the above derivation is that there exists no critical stream power or shear stress that needs to be exceeded in order for bed incision to take place [*Howard*, 1998]. However, it is well known that incipient motion of bed load, which will do most abrasive work on the stream bed, occurs only when a threshold shear stress is exceeded. Several fluvial incision algorithms [e.g., *Densmore et al.*, 1998; *Lavé and Avouac*, 2001; *Sklar and Dietrich*, 1998; *Tucker and Slingerland*, 1997] therefore include such a threshold:

$$\dot{e} = k(\tau - \tau_c)^a \tag{2a}$$

Equation 2a is often simplified to [e.g., *Tucker and Slingerland,* 1997; *Snyder et al.*, 2003]:

$$\dot{e} = k(\tau^a - {\tau_c}^a) \tag{2b}$$

By taking $\tau = K/k\ A^{m/a} S^{n/a}$ and $\tau_c = 1/k\ C_0^{1/a}$, 2b can be rewritten to resemble more closely equation 1:

$$\dot{e} = K\ A^m\ S^n - C_0 \tag{3}$$

We shall refer to algorithm (3) as the 'Excess Stream Power' model.

The above models assume that it is the physical process of detaching bedrock by abrasion, plucking, or cavitation that limits the rate of fluvial incision. Alternatively, one could argue that the supply of material into the river is unlimited but it is the capacity of the river to transport this material that limits incision. A Transport-Limited (as opposed to Detachment-Limited) fluvial incision law can be derived by writing the carrying capacity Q_{eq} of the river as a function of stream power [*Willgoose et al.*, 1991]:

$$Q_{eq} = K_t\ A^{m_t}\ S^{n_t} \tag{4}$$

where, again, K_t is a dimensional constant [$L^{(3\ -\ 2m)}\ T^{-1}$] and m_t and n_t are dimensionless exponents. Incision is calculated by combining (4) with the continuity equation:

$$\dot{e} = \frac{1}{W}\frac{\partial Q_s}{\partial \vec{x}} \tag{5}$$

where Q_s is the amount of sediment in the river (in this model, $Q_s = Q_{eq}$) and $\vec{x}$ is distance in the direction of river drainage.

Several models have been proposed that take the possible role of sediment flux more fully into account. The notion that sediment supply should have a controlling influence on the rate of river incision goes back to the days of Gilbert [cf. review by *Sklar and Dietrich*, 1998]. The influence of sediment flux is twofold: sediments should increase incision capacity by providing abrasive 'tools' to do work on the bed; on the other hand, sediments may cover and protect parts of the bed from the erosive forces of river flow. A recent experimental study [*Sklar and Dietrich*, 2001] has confirmed this two-fold role of sediment flux.

Beaumont et al. [1992] and *Kooi and Beaumont* [1994] derived a fluvial incision algorithm that takes the shielding effect of sediments into account. They describe bedrock incision as a first-order kinetic reaction in which downstream sediment flux variations are inversely proportional to a characteristic length scale L_f and directly proportional to the degree of disequilibrium (the 'undercapacity') in the fluvial sediment flux:

$$\frac{\partial Q_s}{\partial \vec{l}} = \frac{1}{L_f}\left(Q_{eq} - Q_s\right) \tag{6}$$

The equilibrium carrying capacity Q_{eq} is calculated from (4). Combining (6) with the continuity equation (5) gives the incision law for this 'Undercapacity' model:

$$\dot{e} = \frac{1}{W L_f}\left(Q_{eq} - Q_s\right) \tag{7}$$

Note that, for small L_f ($L_f \rightarrow dx$, where dx is the spacing of the numerical model grid), $Q_s \rightarrow Q_{eq}$ and the model collapses into a Transport-Limited Stream Power model. On the other hand, for large L_f ($L_f >> dx$), $Q_s << Q_{eq}$ and the model tends toward a Detachment-Limited Stream Power model. In the original formulation of this model [*Beaumont et al.*, 1992; *Kooi and Beaumont*, 1994], W was included implicitly only because rivers were assumed to have unit width. In order to study the possible influence of varying river width downstream, however, we have chosen to explicitly include W. Also, whereas *Beaumont et al.* [1992] and *Kooi and Beaumont* [1994] implicitly assumed that Q_{eq} is proportional to linear stream power ($m_t = n_t = 1$), we do not restrict ourselves to this case.

Finally, *Sklar and Dietrich* [1998] derived a theoretical model for river incision by abrasion that takes the two opposing controls of sediment into account. They calculate (i) the fraction of channel bed composed of exposed bedrock, which is assumed to depend on the excess transport capacity (Q_{eq} - Q_s), (ii) the particle impact rate per unit area, which depends on sediment flux (Q_s) as well as characteristics such as grain size and saltation length, and (iii)

the volume of material removed per particle impact, which is a function of the particle's kinetic energy. A simplified version of the *Sklar and Dietrich* [1998] model, in which the terms in (ii) other than sediment flux and those in (iii) are assumed constant, is equivalent to an empirical model proposed by *Slingerland et al.* [1997] which predicts the same macro-scale behavior. This 'Tools' model can be parameterized as follows:

$$\dot{e} = \frac{Q_s}{W L_f}\left(1 - \frac{Q_s}{Q_{eq}}\right) \tag{8}$$

In contrast to the Undercapacity model in which $\dot{e}$ decreases linearly with increasing Q_s (and constant Q_{eq}), the Tools model predicts that there is an optimum $Q_s^* = ½\ Q_{eq}$ for which incision rates are maximized, due to the two competing effects of sediment flux in this model.

Very few studies have addressed the question of which of the above formulations (1), (3), (5), (7) or (8) best captures the evolution of fluvial profiles on geological timescales. Most studies that compare model predictions to field data have restricted themselves to the Detachment-Limited Stream Power model and have concentrated on trying to constrain and characterize the parameters K, m, and n [e.g., *Seidl and Dietrich,* 1992; *Seidl et al.*, 1994; *Snyder et al.*, 2000; *Stock and Montgomery*, 1999; *Whipple et al.*, 2000b]. The most comprehensive of these studies [*Stock and Montgomery*, 1999], which used the Upper Lachlan catchment, amongst others, as a test site, found wide variations in the values of K, m, and n that were only partially explained by differences in climate or lithology, as well as strong correlations between these theoretically independent parameters. *Sklar and Dietrich* [1998] also pointed to the strong dependence of K upon the ratio of m/n and showed how subtle disequilibrium in drainage basins may strongly affect estimates of these parameter values. *Slingerland et al.* [1998] compared slope-area relationships predicted by the Stream Power and Tools algorithms, under equilibrium conditions, with data from Taiwan and concluded that these data do not permit discrimination between the different models because sediment flux appeared to scale roughly as a power of drainage area. By comparing stream profiles in the frontal Himalayas to incision rates measured from abandoned fluvial terraces, *Lavé and Avouac* [2001] showed that the rate of incision in these rivers is better described by an Excess Stream Power model than by a simple Stream Power law. Finally, *DeYoung* [2000] compared predictions from a linear Stream Power model and a linear Undercapacity model to observed incision of streams on western Kauai (Hawaii) and concluded that the Undercapacity model predicted the evolution of these profiles, in particular the sections

downstream of major knickpoints, better than the linear Stream Power model. We test all of the above formulations using our data on fluvial incision in the Upper Lachlan catchment. A very similar analysis to ours has recently been performed by *Tomkin et al.* [2003] for the Clearwater River in the Olympic Mountains, NW USA. We will compare our findings for long-term slow incision in the disequilibrium Lachlan catchment to their results for instantaneous rapid incision in the equilibrium Clearwater catchment.

3. STUDY AREA

The Upper Lachlan catchment, that is, the Lachlan River and its tributaries upstream of the town of Cowra (New South Wales), constitutes a ~11,000 km^2 bedrock-dominated drainage basin within the SE Highlands of Australia (Figure 1). The Lachlan River drains the western (inland) slopes of the highlands toward the interior Murray-Darling Basin. The catchment is bounded on its eastern side by the continental drainage divide, formed by the highlands' crest, and to the north and south by the Macquarie and Murrumbidgee River catchments, respectively. Mean annual precipitation in the catchment varies between 620 mm at Cowra and 870 mm at Crookwell and is distributed relatively evenly during the year. In general, the southern spring is somewhat wetter (average precipitation 50-90 mm / month from July – December) than autumn (30 – 50 mm / month from January – June; data from the Australian Commonwealth Bureau of Meteorology, http://www.bom.gov.au/climate/averages/).

In central New South Wales, the SE Highlands form a low-relief plateau with maximum elevations around 1000 m, bounded abruptly to the east by a seaward-facing escarpment. Toward the west, elevations decrease much more gradually. Uplift of the SE Highlands is generally considered to be pre-Cenozoic in age and to be related either to Paleozoic orogeny or to mid-Cretaceous rifting of the Tasman Sea [see reviews by *Bishop and Goldrick*, 2000; *Lambeck and Stephenson*, 1986; *van der Beek and Braun*, 1999; *van der Beek et al.*, 1999]. Much of the relief and drainage patterns of the central highlands were established by the early Cenozoic [*Bishop*, 1986; *Bishop et al.*, 1985]. Both long-term catchment-wide erosion rates and river incision rates for the Upper Lachlan catchment are <10 m $m.y.^{-1}$ [*Bishop*, 1985; *Bishop et al.*, 1985] and are probably limited by the rates of regolith production [*Heimsath et al.*, 2000; *Bierman and Caffee*, 2002].

The bedrock geology of the Upper Lachlan catchment is dominated by Paleozoic metasedimentary and metavolcanic rocks of the Lachlan Fold Belt, intruded by Late Paleozoic

granites (Figure 2). A detailed study of river long profiles [*Goldrick*, 1999], using slope-distance (DS) plots of all 'equilibrium' stream reaches in the catchment (i.e., those reaches that show a linear log distance – log slope relationship), showed that lithology only exerts a second-order control on profile steepness. In general, stream reaches on granites are somewhat steeper than those on metamorphic rock (γ values of 0.97±0.76 for the former and 0.61±0.52 for the latter, where $S = k\, x^{\gamma}$; S = slope; x = distance). The most marked influence of lithology on stream profiles occurs where the east-bank tributaries of the Lachlan River join the trunk stream: the tributaries cut through a hornfels ridge at this junction and are characterized by disequilibrium knickpoints either upstream or downstream of the ridge.

This study focuses on the Tertiary valley-filling lava flows in the Upper Lachlan catchment (Figure 2). These flows, which have been mapped in detail and K-Ar dated at 19-21 Ma by *Bishop* [1986] and *Bishop et al.* [1985], are elongate in map view and usually occur as hilltop cappings as a result of relief inversion. Several features, including their narrow, elongate plan-view geometry, the widespread presence of cross-bedded fluvial sediments at their base and their generally flat tops, allow their recognition as valley-filling flows, thereby permitting the reconstruction of the principal elements of the Early Miocene drainage net and river profiles. Two of the flows, the Bevendale Basalt and the Wheeo Basalt, flowed down to the NW from the continental drainage divide [*Bishop et al.*, 1985]. The Bevendale Basalt follows the Lachlan River valley and the Wheeo Basalt lies adjacent to the present-day Wheeo Creek. Maximum basalt thickness is about 100 m, but generally the basalt remnants do not exceed 40 m in thickness. Post-basalt incision amounts to some 120 m. Due to the initial slightly concave upper surface of the flows, post-basaltic incision has been concentrated at the edge of the basalt remnants, giving rise to a configuration of 'twin lateral streams' that flank the basalt flows on either side (e.g., Merrill and Lampton Creeks along the east-west portion of the Bevendale Basalt; Wheeo and Burrawinda Creeks along the Wheeo Basalt, Figures 2 and 3). These streams have therefore probably only incised through a few meters of basalt before reaching bedrock.

Although most of the tributaries are bedrock-dominated, the Lachlan trunk stream is a mixed bedrock-alluvial river with alluvial stretches increasing in importance downstream. Even in those reaches where the Lachlan is flanked by alluvium, however, the channel bed is formed in bedrock or is known to have been so prior to the extensive sedimentation of the bed by post-European-settlement alluvium. Downstream of the confluence of the Lachlan and Abercrombie rivers at Wyangala Dam (Figure 1), the Lachlan River flows through a narrow gorge-like reach to the bedrock-alluvial transition just upstream of Cowra. The river is

flanked along this gorge reach by well-defined fluvial aggradation terraces up to 30 m above the present stream [*Bishop and Brown*, 1992; *Goldrick*, 1999]. Remnants of a 12.5 Ma valley-filling basalt flow occur 60 m above the stream bed at the junction of the Boorowa and Lachlan Rivers (Figure 1). Terrace elevations decrease downstream and the bedrock-alluvial transition is abrupt: an alluvial fill of ~120 m is recorded in a borehole some 20 km downstream of Cowra (Figure 4). *Bishop and Brown* [1992] suggested that this rapid transition from accelerated incision to aggradation may be explained as a response of the river bed to flexural isostatic uplift of the SE Highlands in response to their denudation, coupled to subsidence of the Murray-Darling basin. Indicators of tectonic activity at the inland highland boundary include its 'range-front' morphology and oversteepened river reaches close to the front [*Goldrick*, 1999; *Goldrick and Bishop*, 1995], as well as a concentration of seismicity [*Lambeck et al.*, 1984]. The bedrock-alluvial transition, which acts as the base-level for the Upper Lachlan catchment, therefore appears to be tectonically controlled and to have remained pinned through time. The rate of incision below the 12.5 Ma Boorowa Basalt just upstream of the bedrock-alluvial transition provides a measure of the rate of Neogene base-level fall as a result of denudational isostasy.

Downstream of Cowra, the Lachlan River flows over a low-gradient interior lowland before terminating in an inland swamp. In flood, the river joins the Murray-Darling river system which drains into the Southern Ocean some 1000 km downstream of Cowra. The Upper Lachlan catchment is thus remote from any influence of Late Cenozoic eustatic base-level variation.

4. DATA

4.1. Present-day and paleo- river profiles

We selected four streams, based on the abundance of flanking basalt remnants, for the simulation of post-basalt incision history. These are the Lachlan River and its upstream continuation into Humes Creek, the twin lateral streams of Merrill Creek and Lampton/Biala Creek that flank the Bevandale Basalt, and Wheeo Creek with its downstream continuation in the Crookwell River (Figure 2).

Present-day stream profiles were digitized from 1:50,000-scale topographic maps [*Goldrick*, 1999]. Basalt outcrops were digitized from the mapping by *Bishop* [1986] and

Bishop et al. [1985]. Elevations of basalt tops were obtained from topographic maps; national mapping trigonometric stations are often located on the tops of the basalt remnants and their elevations are therefore accurately known. Where possible, elevations were checked using high-precision barometric altimetry [*Goldrick*, 1994; 1999]. We expect the basalt-top elevations obtained from the topographic maps to be accurate to within ±10 m; the elevations of the trigonometric stations and those where elevations were measured using an altimeter should be accurate to within ±1 m. Selected elevations of basalt tops (Figure 2) were projected onto the river profiles using a minimum distance criterion. The resulting basalt-top profiles are shown in Figure 5. This figure also shows the elevation of the sub-basaltic surface as mapped by *Bishop* [1986] and *Bishop et al.* [1985].

The elevation difference between the sub-basaltic surface and the present-day river bed provides an estimate of long-term, regional incision rates, as they would have been in the absence of the basaltic valley-filling event [*Bishop*, 1985]. However, a better estimate of the local incision of a stream after the perturbation of its profile by the basalts is given by the elevation difference between the present-day stream bed and the surface defined by the tops of the basalt remnants (supra-basaltic surface; Figure 3). We have therefore reconstructed this supra-basaltic surface as the initial condition for our model simulations.

Whereas the tops of the basalt remnants mark out a relatively clear long profile in the Lachlan River tributaries, there is much more scatter in the elevation data along the trunk stream (Figure 5). The reason for this is undoubtedly the greater erosion of the basalt remnants along the main Lachlan River valley, as also indicated by the greater discontinuity of these remnants along the trunk stream in map view (Figure 2). We can therefore fairly confidently trace a supra-basaltic profile for the Lachlan tributaries but this task is more complicated for the trunk stream, where a number of small basalt outliers are located at high elevations in small tributaries. These can be interpreted in two ways: they are either locally sourced and flowed down the tributaries into the trunk stream (in which case they are unreliable indicators of the elevation of the supra-basaltic surface along the Lachlan River), or they are erosional remnants of parts of the flow that flowed upstream from the trunk stream into the tributaries (in which case all of the basalt tops in the trunk stream are severely eroded and these highest points in the tributaries are the only reliable indicators of the elevation of the supra-basaltic surface). The petrological and geochemical homogeneity of the Bevandale Basalt, as well as the local absence of reliable indicators of flow direction, make it impossible to distinguish between these two possibilities [*Bishop*, 1986; *Bishop et al.*, 1985]. In Figure 5, we therefore show a ‘probable’ maximum elevation of the supra-basaltic surface, which

excludes the outliers but is traced so as to include all the highest basalt elevations along the Lachlan River, as well as a 'possible' maximum elevation which includes the outlying remnants. The effect of this uncertainty on the modeling results is discussed below.

We have few constraints on the initial morphology of the lava snout, which may have had an influence on subsequent incision if a steep initial knickpoint existed. The tops of the most downstream basalt remnants, ~100 km upstream of Cowra, are still ~120 m above the present-day river bed. However, the viscosity of the basaltic Cenozoic lavas of SE Australia is very low and the snouts of the flows therefore probably had relatively low angles. Moreover, incision downstream of the lava flows clearly indicates that the ongoing driving mechanism for incision is the relative base-level fall at the inland highlands' edge.

4.2. Present-day hydraulic variables

In order to evaluate the different fluvial incision algorithms, we need to know how drainage area and, for some of the algorithms, river width vary with distance downstream. Drainage area was obtained from a 9 arc-second Digital Elevation Model (DEM) provided by the Australian Surveying and Land Information Group (AUSLIG), using standard drainage extraction techniques [c.f. *Hurtrez et al.*, 1999]. Although this procedure also allowed us to generate valley long profiles from the DEM data, we chose to use the channel profiles as digitized by *Goldrick* [1999] from the topographic maps because the latter are much more accurate. Contributing drainage areas were calculated at each contour crossing by quadratic interpolation. The resulting area-distance relationship is plotted in Figure 6a. A best-fit power-law through this data is given by:

$$A = 0.18\, x^{1.98} \tag{9}$$

with a regression coefficient $r = 0.97$. Individual streams give results very close to (9) and we therefore believe this close-to-quadratic relationship to be robust.

For the Lachlan River and Wheeo Creek, bankfull widths were measured at each contour crossing on magnified aerial photograph stereo models with a nominal scale 1:40,000, using vernier calipers and correcting for scale distortion due to different terrain heights (measurements accurate to 0.1 mm, giving a nominal accuracy of the channel width measurements of ~4 m). This procedure allows us to track the general increase in river width downstream but filters out shorter wavelength variations that may be due to lithological

changes [e.g., *Brocard*, 2002]. A best-fit regression on this data (Figure 6b) gives a close-to-square-root dependence of width on drainage area:

$$W = 0.012\, A^{0.41} \tag{10}$$

With $r = 0.65$. However, the data for the two streams are not collinear; taken individually, the Lachlan river relationship is $W = 4\times10^{-4}\, A^{0.55}$ ($r = 0.73$) and the Wheeo Creek data give $W = 10^{-3}\, A^{0.53}$ ($r = 0.70$). In spite of this discrepancy, we will use equation 10 for most of our model runs, for the sake of numerical simplicity.

Figure 6c and d show the relationship between local stream slope, area, and distance. Slopes were calculated for the inter-contour stream reaches upstream and downstream of each contour crossing and averaged to give a value at that contour crossing. The data show a large scatter that illustrates the fact that none of the streams studied is in equilibrium [*Goldrick*, 1999]. On Figure 6d, the empirical critical slope-area relationship for the bedrock-alluvial transition in Olympic Mountains (NW USA) drainage basins $S_t = 70\, A^{-0.5}$ [*Montgomery et al.*, 1996] is also plotted. Although there is no *a priori* reason why the Lachlan catchment, with its very different climate, lithology, and vegetation should follow the same rule, the data generally plot relatively close to the above relationship.

5. MODELING APPROACH

Our aim in modeling the post-Early Miocene incision of the Upper Lachlan River and its tributaries is to test how well the various fluvial incision algorithms predict the present-day river profile, and the parameter values of the best fit. Conceptually, river incision in this catchment is driven by two independent controls: continuous relative base-level lowering at the bedrock-alluvial transition near Cowra, caused by denudational isostatic rebound of the highlands and subsidence of the interior basins [*Bishop and Brown*, 1992], and disturbance of the river profiles by the Early Miocene valley-filling basalts.

The starting condition for our numerical model is given by the elevation of the supra-basaltic profile shown in Figure 5. This profile is linearly interpolated to a uniform 500-m grid spacing. We then let the profile evolve through time by integrating the fluvial incision algorithms (1), (3), (5), (7) or (8). For the Stream Power and Excess Stream Power models (equations 1,3 and 5), this is achieved using a fourth-order Runge-Kutta finite-difference technique with adaptive time-stepping [*Press et al.*, 1992]. Local contributing drainage area is

calculated from (9), local slopes are estimated by central differences. The area-distance relationship is kept constant through time, implying that the drainage net has not changed significantly since the Early Miocene. Although some changes to the drainage net may have taken place in detail, as indicated by tributary streams of the Lachlan River cutting through the Wheeo Basalt (Figure 2), the general drainage pattern has remained remarkably stable [*Bishop*, 1986; *Bishop et al.*, 1985].

For the Undercapacity and Tools models, we track sediment load Q_s downstream by solving (6) and its equivalent for the Tools model, and then calculate incision at each time step from (7) or (8). The sediment load carried by the river is not only produced by the integrated upstream incision; material is also washed in from the slopes and tributaries. We therefore add a sediment flux equal to the catchment-wide denudation rate ε times the incremental increase in drainage area at each point:

$$Q_{s_{(x)}} = \int_0^x W_{(x')}\, \dot{e}_{(x')}\, dx' + \varepsilon\, A_{(x)} \tag{11}$$

We adopt a mean long-term catchment-wide denudation rate ε of 4 m m.y.$^{-1}$ [*Bishop*, 1985]. This procedure supposes that denudation rates have remained relatively constant since the Miocene [cf. *Bishop*, 1985] and that sediment is routed efficiently to the trunk stream.

All models are run for 21 m.y., the best estimate of the age of the basalts. The upstream boundary is kept fixed for all streams. This is justified by the apparent minimal incision of the basalts close to the drainage divide [*Bishop et al.*, 1985]. The downstream boundary condition for the Lachlan River is one of constant lowering at a rate of 4.6 m m.y.$^{-1}$, obtained by extrapolation of the incision rate inferred from the elevation of the base of the 12.5 Ma Boorowa Basalt above the present-day river bed. The Lachlan tributaries are tied to the trunk stream by the lowering of their tributary junctions, which is used as their downstream boundary condition.

We explore the parameter space for all algorithms by either systematically varying the parameter values (for models with one or two independent parameters) or by Monte Carlo sampling of the parameter space (for models with more than two independent parameters). Model performance is assessed by calculating root-mean-square (RMS) misfits between predicted and observed incision for all streams. We report an overall weighted mean RMS misfit by weighting the individual stream misfits by the number of mapped basalt tops. We choose to apply this weighting criterion because on the one hand, weighting by length would put excessive emphasis on the Lachlan trunk stream (for which, moreover, incision is

essentially unconstrained up to 100 km upstream of Cowra); on the other hand, weighting by the number of contour crossings would put too much importance on the steep tributary streams. We also evaluate model performance by examining systematic errors in the model predictions. To do this, we linearly regress the difference between modeled and observed incision against distance downstream; the slope of the regression line (s) is a measure of structure in the misfit. The misfit structure is clearly non-linear along the profiles (cf. Figure 8) and a simple linear regression therefore does not resolve the misfit function very well. However, we are not interested here in the fine detail of the misfit structure and use s simply as a first-order and conservative indicator of model fit.

6. MODELING RESULTS

In the following, we test the different models starting from an initial condition given by the 'probable maximum' elevation of the supra-basaltic surface. The influence of this choice and the uncertainty it induces in the results is treated in the Discussion section.

6.1 Detachment-Limited Stream Power Model

As a first and very simple approach, we employ a linear Stream Power law (equation (1) with $m = n = 1$) to model stream profile evolution in the Upper Lachlan catchment. We do not predict this to be a particularly appropriate model, but it provides a simple starting point with only one variable (K) and gives some general insights. A general 'best fit' for this model is achieved for $K = 2\times10^{-12}$ $m^{-1}y^{-1}$ (Table 1). However, the weighted mean RMS misfit for this best-fit model is 80 m and the misfit shows significant structure (s = 1.36 m km^{-1}) implying that the model severely underpredicts incision in the headwaters and overpredicts incision downstream. Given that mean incision along the four streams is 121 m, this is clearly an unsatisfactory model. Figure 7 shows the predicted present-day long profiles from this model (compared to nonlinear Stream Power models) and Figure 8 shows the misfit.

Next, we study the controls of the exponents m and n on the predicted incision. We do this by systematically varying the values of both exponents between 0 and 2. For each combination of m and n, we estimate an initial value for K:

$$K^*_{(m,n)} = K^*_{(1,1)} \, \overline{A}^{(1-m)} \, \overline{S}^{(1-n)} \tag{12}$$

where $K^*_{(1,1)}$ is the best-fit K value for the linear Stream Power model (2×10^{-12} $m^{-1}y^{-1}$), and $\overline{A}$ and $\overline{S}$ are the mean contributing area and slope for the Upper Lachlan catchment, respectively. A subsequent search around this value showed that this initial guess is a good estimate of the best-fit K, which deviates by less than 30% from the initial guess. Figure 9a shows how RMS misfit and misfit structure vary as a function of m and n.

Models that fit the incision data best are characterized by m = 0.3-0.4 and n = 0.7-1.0; these models have RMS misfits of 42-54 m. Model predictions and misfits are more sensitive to changes in m than in n. Models with m / n ratios > ~0.4 ($n \leq 1$) are characterized by positive structure in the misfit function, that is, they underpredict incision in the headwaters and overpredict incision downstream; the opposite is true for models with $m / n < 0.4$. In general, the best-fit m and n values suggested by our modeling are consistent with theoretical predictions of incision being proportional to either unit stream power or basal shear stress (cf. Section 2). They do not, however, allow discrimination between these two models. The shear stress model (m = 0.3; n = 0.7; $K = 7.0\times10^{-7}$ $m^{0.4}$ y^{-1}) predicts the lowest misfit (42 m); the unit stream power model (m = 0.4; n = 1; $K = 4.7\times10^{-7}$ $m^{0.2}$ y^{-1}) has a somewhat higher RMS misfit (53 m) but shows least structure (s = -0.09 m km^{-1}; Figure 8; Table 1).

In general, the models predict incision in the headwaters and along the tributaries reasonably well, as they do for incision in the downstream reaches of the Lachlan River. It is the central reach of the Lachlan River, where the profile has been most disturbed by valley-filling basalts (and where our data constrain the paleo-profile best), that poses most problems, even when using our conservative 'probable maximum supra-basaltic surface' as a starting condition.

6.2 Excess Stream Power Model

We have tried to improve on the Stream Power Model results by including a threshold for incision C_0. The Excess Stream Power algorithm (3) contains four free parameters that may be varied independently: K, m, n, and C_0. We have conducted a Monte-Carlo search through this parameter space by randomly sampling m and n values between 0 and 2 with a sampling interval of 0.1. An initial K^* is estimated from (12); because the Excess Stream Power model leads to less incision than the Stream Power model for the same parameter values, K is allowed to vary up to an order of magnitude above this initial guess. Finally, C_0 is sampled between 5×10^{-7} and 5×10^{-5} m y^{-1}. Results are shown in Figure 10a. None of the models provides very satisfying fits; best fitting models have weighted-mean RMS Misfits of 60-70

m. As for the Stream Power model, these models are characterized by $m \leq 0.5$ and $0.5 \leq n \leq 1$. Best-fitting models also have K close to K^*, while no strong dependence on C_0 appears. A concentration of models with RMS Misfits around 120 m is apparent in Figure 10a; these models have parameter combinations that lead to negligible incision. Note that these models are mostly characterized by high ($>10^{-5}$ m y^{-1}) C_0 values.

We have conducted a more systematic search using the combinations of m and n that give the most satisfactory results for the Stream Power model; that is: m = 0.3-0.4 and n = 0.7-1. Figure 10b shows RMS misfits as a function of K and C_0 for these two combinations of m and n. A comparison of the figure with the Stream Power Model results in Figure 9 shows that in all cases, the RMS misfits of the Excess Stream Power models are higher than those of the corresponding (same m and n values) Stream Power models. Misfit contours tend towards a minimum for $C_0 \rightarrow 0$ and $K \rightarrow K^*_{(m,n)}$. Moreover, practically all the models tested produce significant positive structure in the misfit function ($s > 0$), that is, they severely underpredict incision in the headwaters. This is because Stream Power generally increases downstream (except for models where $n >> m$); therefore, including a constant threshold strongly diminishes incision in the headwaters, whereas the effect is less strong downstream. Values of s decrease for increasing C_0, reflecting the increasing influence of the threshold on incision downstream. We conclude from these results that, at least in the Lachlan catchment, a threshold for incision is not resolvable and its inclusion into a fluvial incision algorithm is not required to model fluvial incision adequately.

6.3 Transport-Limited Stream Power Model

For testing the Transport-Limited Stream Power model, we take the same approach as for the Detachment-Limited Stream Power model, that is, we first find a best-fit K_t value for the linear model and then search the m_t, n_t space for a best-fit solution, adapting K_t as in (12). River width, which enters in equation (5), is calculated from the contributing drainage area using (10). The resulting plots of RMS Misfit and Misfit structure are shown in Figure 9b. Figure 11 shows predicted present-day river profiles for selected models; RMS Misfits and s-values for these models are reported in Table 1.

Best-fit Transport-Limited Stream Power models have RMS misfits of 45-50 m and very little structure in the solutions ($s < 0.05$); these fits are comparable to the best-fit Detachment-Limited Stream Power models. However, these best-fit models are found for m_t = 1.2-1.3 and n_t = 0.6-0.7, values that are not easily interpreted in terms of physical models for

fluvial sediment transport or incision. Predicted misfits are less sensitive to m_t than for the Detachment-Limited model. In contrast, misfit structure is strongly sensitive to m_t: all models with $m_t \leq 1$ have negative *s*-values, that is, they overpredict incision in the headwaters compared to downstream incision.

Due to the strong diffusive component in (5), predicted present-day river profiles are very smooth; the initial irregularities in the river profiles have been completely removed. This is in sharp contrast to the predictions of the Detachment-Limited Stream Power models, where these irregularities persist in the present-day profiles, and are even enhanced for certain combinations of *m* and *n* (compare Figures 7 and 11). It appears that the Detachment-Limited models predict too much irregularity in the present-day profiles, whereas the Transport-Limited models predict too little; better solutions may possibly be found by employing 'hybrid' models which take a more complex role of sediments into account.

6.4 Undercapacity Model

The first 'hybrid' model that we test is the Undercapacity model. Initial model runs with this model are conducted to test the initial formulation of *Beaumont et al.* [1992] and *Kooi and Beaumont* [1994], that is, a linear dependence of carrying capacity on drainage area and slope ($m_t = n_t = 1$ in equation 4) and a constant river width (here taken to be 50 m, an approximate average width for the rivers we are studying). This description limits the number of free parameters to two: the transport parameter K_t and the length scale for fluvial incision L_f. RMS misfits and misfit structure for these models are plotted in Figure 12a as a function of these two parameters. The figure shows that best-fit models are obtained for $K_t = 10^{-5}$ m y^{-1} and $L_f \leq$ 1 km. The RMS-misfit plot shows a clear minimum for very low L_f values that are close to the numerical grid spacing of 500 m. This means that the best-fit constant-width Linear Undercapacity models are those that mimic the behavior of Transport-Limited Steam Power models. Moreover, misfit structure is (strongly) positive for practically all models tested. Figure 13 shows predicted present-day stream profiles for this model; note that the best-fit constant-width model predicts a profile that is nearly indistinguishable from that predicted by the best-fit Transport-Limited Stream Power model in Figure 11.

Next, we test Linear Undercapacity models in which river width is allowed to vary downstream following (10). Results for this model are much more satisfactory than for the constant-width model: the RMS-misfit plot (Figure 12b) shows a clear minimum (RMS misfit = 56 m) for $K_t = 10^{-5}$ m y^{-1} and $L_f = 30$ km (that is, a finite L_f significantly larger than the numerical grid spacing). RMS-misfit contours are sub-parallel and have a positive slope in

the $K_t - L_f$ plot, demonstrating that the mean amount of incision along the river profiles is controlled by the ratio between these two parameters [*van der Beek and Braun*, 1998]. For any ratio of K_t / L_f, the distribution of incision along the profile is controlled by L_f: high L_f values tend to concentrate fluvial incision downstream, whereas it spreads upstream for lower L_f values [*Kooi and Beaumont*, 1994; *van der Beek and Braun*, 1998; 1999]. This is demonstrated by the misfit-structure plot, which shows positive *s*-values for L_f > ~20 km (and constant K_t / L_f) and negative *s* for smaller L_f.

Finally, as there is no *a-priori* reason why the relationship between carrying capacity, drainage area, and slope should be linear, we also test Undercapacity models based on non-linear forms of (4). These models contain four free parameters: K_t, L_f, m_t, and n_t. These are, however, not strictly independent: we know that acceptable fits will only be attained for certain K_t / L_f ratios and certain combinations of K_t, m_t, and n_t. We have, therefore, developed a Monte Carlo sampling scheme in which m_t and n_t are sampled randomly between 0 and 2 (with a sampling step of 0.1) and L_f is sampled between 1-100 km. An initial guess of K_t is then made:

$$K^{*}_{t(L_f,m_t,n_t)} = \left(K_t / L_f\right)^{*}_{(1,1)} L_f \, \overline{A}^{(1-m)} \, \overline{S}^{(1-n)} \tag{13}$$

in which $(K_t / L_f)^{*}_{(1,1)} = 10^{-5}/3\times10^{4}$ y^{-1} is the best-fit K_t / L_f ratio for the Linear Undercapacity model. The actual K_t is allowed to vary within an order of magnitude around this initial guess. Results of the Monte Carlo sampling are presented in Figure 14, which shows results for 856 runs out of 1500 Monte Carlo runs performed; other models have parameter combinations which lead to runaway incision and develop numerical instabilities. There appears to be a strong control of m_t on the solutions: best-fit models consistently have $0.5 < m_t \leq 1$ and minimum RMS misfits increase rapidly for $m_t > 1$. All models with $m_t \leq 0.5$ develop numerical instabilities; these models are characterized by large K_t leading to runaway incision in the headwaters. Results are less dependent on n_t, although best-fit models have $n_t \leq 0.5$ and minimum RMS misfits increase regularly for larger n_t. The dependence on L_f and K_t appears to be relatively weak; relatively good-fitting models (RMS ≤ 50 m) are found for all values of these parameters that we tested, although there appears to be a slight preference for models with intermediate values of L_f ($5 \leq L_f \leq 50$ km). Predicted present-day stream profiles for the overall best-fitting Undercapacity model (RMS misfit = 38 m) are shown, together with the Linear Undercapacity results, in Figure 13.

The tendency of the model to prefer low n_t-values appears to be caused by the necessity to minimize incision in the headwaters. Note that in the Undercapacity model, rivers

are most 'aggressive' when $Q_{eq} >> Q_s$, that is, when they carry little sediment. This situation is most likely to occur in the headwaters. An alternative description, which takes the 'tools' effect of sediment into account, may provide similar results for n_t-values that are easier to interpret.

6.5 Tools Model

The most general forms of the Tools and Undercapacity model descriptions are very similar (compare Equations 7 and 8). The Tools model is controlled by the same four parameters as the Undercapacity model: K_t, L_f, m_t, and n_t. In testing the Tools model we therefore take the same approach as for the Undercapacity model: we first test a linear version of the model with $m_t = n_t = 1$ and then perform a Monte Carlo search of the full parameter space, estimating an initial value for K_t as above. Search results for the Linear Tools model are presented in Figure 15a, for both constant-width and variable-width descriptions. As for the Undercapacity model, the constant-width version of the model finds best-fit solutions for very low values of L_f, close to the numerical grid spacing. In contrast to the Undercapacity model, however, these results do not change significantly when adopting a variable-width model: best-fit L_f values are still <5 km.

This preference for low L_f values is a characteristic of all Tools models that we tested, as shown by the plot of Monte Carlo search results in Figure 15b. Relatively acceptable fits (RMS misfit ≤ 60 m) are only found for models with $L_f \leq 5$ km; all models with $L_f > 10$ km have RMS misfits > 100 m. This strong preference for low L_f values can be explained because, if the river does not incise sufficiently in its headwaters, Q_s never increases to a point where incision becomes efficient; the model river is stuck in a low transport – low incision mode.

The dependence of Tools model results on the other parameters (m_t, n_t, and K_t) is similar to that of the Undercapacity model: the model prefers values of m_t close to 1, $n_t \leq 1$, and model results are not strongly influenced by the choice of K_t. Note that results for the Tools model are strongly non-linearly dependent on the parameter values because of the strong non-linear dependence of incision rate on values of Q_s and Q_{eq}. Very small variations in parameter values may drive a model from predicting negligible incision to predicting runaway incision and becoming numerically instable. Figure 15b therefore only represents results of 702 model runs out of 2000 tested. Overall, the results are clearly less satisfactory than for the Undercapacity model: RMS values for the Tools model are consistently higher than for the corresponding (same parameter values) Undercapacity model and the strong

preference for very low L_f values means that best-fit Tools models are those that mimic the Transport-Limited Stream Power model.

7. DISCUSSION

A comparison of the best-fit predictions for each model formulation above shows that all models are capable of predicting amounts of incision that fit the observed amounts reasonably well (RMS misfits < ~50 m; cf. Table 1). None of the models stands out as predicting incision significantly better than the others. However, some of the best-fit models have parameter combinations that appear unrealistic, or at least difficult to explain physically. If we require from our models that they include a description of transport capacity or bedrock incision that is a function of total stream power, stream power per unit width, or shear stress (that is, we only consider models based on equations (1) or (4) with m / n ratios of 0.4 - 1) then the Transport-Limited Stream Power model and the non-linear versions of the Undercapacity and Tools models provide unsatisfactory results. Moreover, some models provide best-fit results for parameter combinations that lead them to mimic the behavior of other models. The Excess Stream Power model gives best-fit results for $C_0 \rightarrow 0$ so that it resembles a Detachment-Limited Stream Power model. The constant-width version of the Undercapacity model and all Tools models give best-fit results for L_f close to the model grid spacing such that their behavior resembles that of the Transport-Limited Stream Power model. Given the above, the two models which give the most satisfying results appear to be the Detachment-Limited Stream Power model and the Linear Undercapacity model (including a variable width term). These results suggest that (1) a critical stream power for fluvial entrainment is not resolvable within the Upper Lachlan catchment; (2) transport-limited behavior alone does not adequately describe fluvial incision within the catchment; and (3) the Undercapacity model, with a linear dependence of incision capacity on sediment flux, provides a better description of fluvial incision within the catchment than the Tools model. These results merit some more detailed discussion; first, however, we will test the sensitivity of our model outcomes on initial conditions and compare our results to previous findings.

7.1. Parameter sensitivity and inter-stream variability

Even the two best-performing models (Detachment-limited Stream Power and Undercapacity) provide only moderately good fits to the observed incision. Best-fit parameter combinations

have RMS misfits between 42 and 55 m, implying that they explain less than two-thirds of the total incision. Our models do not take into account the potentially important controls on river incision and profile development that may be exerted by orographic precipitation and downstream fining of sediments [*Brocard*, 2002; Gasparini *et al.*, 1999; *Lavé and Avouac*, 2001; *Roe et al.*, 2002; *Sklar and Dietrich*, 1998]. However, we do not expect these effects to be important in the low-relief setting that we study. The reason for this relatively poor fit appears to be that best-fit parameters vary significantly between the individual streams. Figure 16 shows how RMS misfits vary with the value of the input parameters for the Stream Power and Undercapacity models for individual streams. The figure shows that best fits are obtained for the Lachlan River (as well as Lampton and Merrill Creeks) for parameter values that are 3-5 times larger than those that provide a best fit to the Wheeo Creek data. The overall best-fit model is therefore always a compromise between these two.

This discrepancy between individual streams is dependent on the choice of initial conditions. The Lachlan River and its tributaries need to incise much more than Wheeo Creek, even for the conservative 'probable maximum' supra-basaltic surface used as the initial condition thus far. Recall that the amount of incision is well constrained along Wheeo Creek whereas only a minimum estimate is possible along the Lachlan River. Using the 'possible maximum' supra-basaltic surface as initial condition, therefore, aggravates the problem of discrepancy between the different streams and increases the RMS misfit for all models (Figure 16).

We have performed a sensitivity analysis of the parameter values on the initial conditions by conducting a systematic search for best-fit *m*-*n* combinations for the Stream Power model and for best-fit K_t-L_f combinations for the Undercapacity model, using the 'possible maximum' supra-basaltic surface as a starting condition. The results show that the parameters are relatively robust with respect to the initial conditions. For the Stream Power model, best fits are found for the same values of *m* and *n* as before, with best-fit *K* values approximately 1.5 times higher. For the Undercapacity model, a best fit is found for L_f = 30 km (the same value as previously) and $K_t = 1.5\times10^{-5}$ m y^{-1}, 1.5 times higher than for the 'probable maximum' initial conditions. RMS misfits are, however, systematically higher than for corresponding models using the 'probable maximum' supra-basaltic surface as initial conditions (Table 1).

The observed discrepancy in best-fit parameter values for individual streams suggests that bedrock lithology may control incision rates in our study area. Although *Goldrick* [1999] suggested that lithology only has a modest influence on river profile development in the

Upper Lachlan catchment, he also showed that Wheeo Creek, which flows mainly over Wyangala Granite, has a significantly larger concavity index than the other streams that we studied and that flow mainly over low-grade metamorphics of the Adaminaby Group (cf. Figure 2). Therefore, for the same contributing drainage area or same distance downstream, local slope is higher in Wheeo Creek than in any of the other streams (Figure 6) and stream power will also be higher. In order to test whether lithological influence plays a role, and to estimate to what extent it may influence parameter values, we have designed models in which the values of the input parameters are allowed to vary according to whether the rivers flow over granites or metamorphic rocks. Stream reaches flowing over each of these lithologies are identified from the digitizing by *Goldrick* [1999] and parameter values are adapted for both lithologies until a best-fit river profile is obtained. Figure 17 shows results for a Detachment-Limited Stream Power model (m = 0.4, n = 1) and a Linear Undercapacity model. Best-fit results are obtained by allowing parameters to vary by a factor of 3-5 between the two lithologies considered; RMS misfits for these best-fit models are significantly improved compared to the single parameter models (35 *vs* 53 m for the Stream Power model; 41 *vs* 55 m for the Undercapacity model, cf. Table 1). Although we let the parameter values vary freely as necessary to obtain a best-fit, the relative parameterizations for the two-lithology models match our expectations, that is, the Adaminaby Group metamorphics are more erodible than the Wyangala Granite. From this test we conclude that lithological variation is an important factor controlling incision in the Upper Lachlan catchment and that even rather subtle variations in lithology may be expressed by significant (3-5 fold) variations in controlling parameters.

The above conclusions apparently deviate from those of *Goldrick* [1999], who suggested minimal lithological control, but note that he studied present-day river profiles only, whereas we look at river incision. Inspection of Figure 17 shows that both observed and predicted present-day river profiles are relatively complex and contain lithological knickpoints as well as disequilibrium knickpoints inherited from the initial stream profiles and transferred upstream. In particular, the very steep reaches at the downstream end of the tributaries are maintained both by strong incision in the Lachlan trunk stream and by lithological variation, as envisaged by *Goldrick* [1999]. In such a complex and disequilibrium setting, it is extremely difficult to unambiguously identify lithological control on profile form.

7.2 Comparison with previous results

Although our study is more complete than previous ones, we can compare at least some of our results with previous studies. In particular, we can compare our results for the Stream Power model with those of *Stock and Montgomery* [1999], who used the Lachlan River and Wheeo Creek, amongst others, as test cases. *Stock and Montgomery*'s [1999] best-fit parameter values for the Lachlan River are m = 0.3-0.5 and n = 0.4-1; for m = 0.4, n = 1 they find a best-fit $K = 4.3\times10^{-6}$ $m^{0.2}$ y^{-1}. For Wheeo Creek they suggest their estimates of m and n to be unreliable; for m = 0.4, n = 1 they find $K = 4.4\times10^{-7}$ $m^{0.2}$ y^{-1}. Our best-fit m and n values therefore corroborate theirs, our best-fit K is close to their estimate for Wheeo Creek but significantly lower than their best-fit K for the Lachlan River. These differences are undoubtedly due to the different boundary conditions that we impose on our models compared to *Stock and Montgomery* [1999]: whereas they imposed a base-level drop at their most downstream profile point, we impose it at the bedrock-alluvial transition from where it is communicated >100 km upstream. *Stock and Montgomery* [1999] also used the sub-basaltic profile as their initial condition whereas we use the supra-basaltic surface, for reasons we have explained above. Given these discrepancies, the relative coherence between our parameter estimates is quite remarkable, although we find their very high K value for the Lachlan River puzzling. In our model, as compared to *Stock and Montgomery* [1999], the Lachlan River needs to incise much more and incision is partly driven by a base-level drop that is far downstream, yet best fits are obtained for a K that is 4-10 times lower than theirs.

A quite similar analysis to ours has recently been performed by *Tomkin et al.* [2003] for the Clearwater River in the Olympic Mountains (NW USA). The major difference between the two study areas is that the Clearwater River is believed to be in equilibrium [*Pazzaglia and Brandon*, 2001] whereas the Lachlan clearly is not. Also, long-term incision rates are two orders of magnitude larger in the Clearwater than in the Lachlan. *Tomkin et al.* [2003] tested whether best-fit parameter combinations for the five incision models also tested here, plus an alternative 'sediment-limited' model, were physically plausible (as expressed by m / n ratios that conform to theory) and found that none of the models they tested provided an adequate fit. Our findings are somewhat more optimistic than theirs in that at least some models or model combinations appear to describe long-term incision in the Lachlan catchment reasonably well. *Tomkin et al.* [2003] noted that the tendency for most of the models to prefer very low or even negative m values may be explained because the largest discharge events would tend to flood the downstream reaches of the river and thus lose their incision capacity downstream. Within the Lachlan catchment, with its relatively small

temporal variations in discharge, flooding is much less frequent and incision therefore more directly related to discharge.

7.3. Implications for fluvial incision models

A principal goal of this study was to test fluvial incision algorithms in a well-constrained natural setting, in order to aid the selection of algorithms to include in numerical surface process models (SPMs). From this example alone, we would argue that Excess Stream Power, Transport-Limited Stream Power, or Tools models fail to describe fluvial incision appropriately on regional scales. We note, however, that many more examples of the kind we have studied will be needed to corroborate this conclusion. Based on our data, we would argue that either simple Detachment-Limited Stream Power models or Linear Undercapacity models appear to be the most appropriate choices for inclusion in numerical SPMs. The latter model should, however, include a width term that varies with drainage area in order to introduce non-linearity in the area dependence [see also *Whipple and Tucker*, 2002].

Our conclusion that a threshold for incision is not resolvable in the Lachlan catchment may be influenced by our implementation of a linear form of the Excess Stream Power model (equations 2b and 3), although *Tomkin et al.* [2003], who use the fully non-linear formulation (2a), note a similar vanishingly small threshold. In contrast, *Baldwin et al.* [2001] and *Snyder et al.* [2003] suggest that a threshold shear stress may play a major role controlling river incision, and may notably explain the observed extreme variations in incision rates between actively uplifting and tectonically quiet regions, without similarly large differences in relief [see also *Pazzaglia et al*., 1998]. The approach of these authors is somewhat different, however, in that they express the erosion coefficient K of the Stream Power model as a product of three factors encompassing hydraulic, climatic, and threshold shear stress parameters respectively. The climatic parameters include a stochastic representation of runoff events. Testing such a model can only be done in a region with spatially and / or temporally varying relief and runoff parameters and where, moreover, these variations can be constrained. In the absence of such data, implementing such a model with temporally constant runoff parameters would simply come down to employing a Detachment-Limited Stream Power model with greatly reduced effective K. Moreover, predicted relationships between river gradient and incision rate using the stochastic runoff – threshold model are equally well explained by models including sediment covering of the bed [*Snyder et al.,* 2003].

In a way, it is surprising that the Transport-Limited Stream Power model does not give more satisfactory results in the Upper Lachlan catchment. It has been argued that transport-

limited behavior should be favored in geomorphic systems that are in a declining state [*Baldwin et al.*, 2001; *Pazzaglia et al.*, 1998; *Whipple and Tucker*, 2002], such as is the case in the stable post-rift setting of the SE Australian highlands. Moreover, it has been argued that mixed bedrock-alluvial rivers such as the Lachlan should be transport-limited systems [*Howard*, 1998; *Whipple and Tucker*, 2002]. Finally, transport-limited behavior has been demonstrated to occur in equilibrium rivers in moderately active orogenic settings such as the Italian Apennines and the French western Alps [*Brocard*, 2002; *Talling and Sowter*, 1998]. However, the relatively resistant lithologies and generally low stream power within the Upper Lachlan catchment, as well as the long-term persistence of disequilibrium knickpoints [*Bishop and Goldrick*, 2000; *Goldrick*, 1999] argues against purely transport-limited behavior, in which knickpoints would rapidly decay away [*Gardner*, 1983; *Whipple and Tucker*, 2002].

The poor performance of the Tools model with respect to the Undercapacity model is also surprising, given that the dual role of sediments (providing tools to abrade the bed on one hand, protecting it on the other) is conceptually more aptly described by the Tools model than by the Undercapacity model. A possible solution to this paradox may be found in the experimental results of *Sklar and Dietrich* [2001], which show that maximum incision rates occur for relatively low sediment fluxes ($Q_s^* \approx 0.1\ Q_{eq}$ as estimated from their Figure 4, instead of $Q_s^* = 0.5\ Q_{eq}$ as predicted by the Tools model) so that the shielding role of sediments (taken into account by the Undercapacity model) dominates for most sediment flux values.

Although the Detachment-Limited Stream Power model predicts the best-fitting incision profiles of all the models we tested, it has a conceptual weakness in that it predicts that rivers will always incise. Therefore, the Detachment-Limited Stream Power model may be useful to study incision on a local scale [e.g., *Kirby and Whipple*, 2001; *Snyder et al.*, 2000] but its use on regional scales [e.g., *Finlayson et al.*, 2002; *Royden et al.*, 2000] appears problematic. In numerical SPMs the problem may be circumvented by combining Detachment-Limited and Transport-Limited Stream Power algorithms, with the one that predicts the lowest incision being taken as the rate-limiting process [e.g., *Densmore et al.*, 1998; *Tucker and Slingerland*, 1994; *Whipple and Tucker*, 2002]. Alternatively, "hybrid" formulations such as the Undercapacity model implicitly predict transitions from one to the other behavior to take place along the streams. Figure 18 shows the predicted present-day 'undercapacity' (defined as $1 - Q_s/Q_{eq}$) along the streams we modeled. All streams show a transition from detachment-limited behavior ($Q_s << Q_{eq}$; $1 - Q_s/Q_{eq} \rightarrow 1$) upstream to

transport-limited behavior ($Q_s \rightarrow Q_{eq}$; $1 - Q_s/Q_{eq} \rightarrow 0$) downstream. The location and abruptness of this transition depends on L_f. The variable-lithology model moreover shows transitions between the two modes of behavior that are lithology dependent, suggesting that lithological knickpoints are not solely related to changes in bedrock erodibility, but may reflect a change in behavioral mode of the river.

The use of combined Detachment- and Transport-Limited models has led to the notion that many rivers may be at a 'threshold', in that they are exactly adjusted to transport their sediment load in equilibrium conditions, but their transient response to base-level drops is detachment-limited. *Whipple and Tucker* [2002] showed how such threshold rivers would operate theoretically. *Brocard* [2002] provides evidence that western Alpine rivers indeed demonstrate such behavior, as they show characteristics of transport-limited systems where they are in equilibrium but they become detachment-limited when pushed out of equilibrium. We suggest that similar processes may be operating in the Lachlan catchment, but on much longer timescales, as the rates of incision are much lower and river response time therefore much longer.

Whether such transient 'threshold' channels, which may be very common, are better described by coupling Transport- and Detachment-Limited Stream Power models or by 'hybrid' models such as the Undercapacity model, will depend on (1) whether transitions from detachment-limited to transport-limited behavior are abrupt or gradational, and (2) whether similar parameter values (in particular m - m_t and n - n_t values) control the two laws. The first question will require detailed fieldwork as well as an understanding of how to discriminate between detachment-limited and transport-limited stream reaches in the field; a partial answer to the second question may be given by comparisons of river concavity indexes for streams in which incision is supposed to be either detachment- or transport-limited [e.g., *Snyder et al.*, 2000; *Talling and Sowter*, 1998]. These data suggest that there may not be a significant difference in exponent values between the transport and detachment laws [cf. review by *Whipple and Tucker*, 2002] and, therefore, it may be possible to capture 'hybrid' river behavior in a single algorithm.

CONCLUSIONS

From our forward models of stream profile development in the Upper Lachlan catchment, we can draw the following conclusions:

For all of the five fluvial incision algorithms tested we can find parameter combinations that lead to reasonable estimates of fluvial incision. For some of the models, however (notably the Transport-Limited Stream Power model and the non-linear Undercapacity and Tools models), these parameter combinations appear to have no physical significance, whereas for some models the best-fit parameter combinations are such that these tend to mimic other models (best-fit Excess Stream Power models behave as simple Detachment-Limited Stream Power models; best-fit Tools models behave as Transport-Limited Stream Power models). Of the five algorithms tested, the Detachment-Limited Stream Power model and the linear Undercapacity model appear to describe fluvial incision best. The latter model needs to include a river width term that varies as a function of drainage area.

The uncertainty in initial conditions does not strongly influence the model outcome. Using initial conditions that maximize the required amount of incision lead to parameter values that are approximately 1.5 times higher than those for a more conservative estimate of incision. There are, however, large differences between the different streams we studied, which appear to be related to lithological variation. Models including lithological variation along the different streams provide much better fits to the data than single-lithology models and involve 3-5 fold variations in parameter values for the different lithologies.

Acknowledgements

This study was funded in part by an *Alliance* Anglo-French collaboration grant to both authors. We thank Geoff Goldrick for supplying the GIS data and Pascale Leturmy for her aid in drainage extraction. Greg Tucker provided us with preprints of his recent papers and pointed out the potential importance of transport-limited behavior. PvdB thanks Chris Beaumont for hospitality and discussions during a short visit in an early stage of this project. Leonard Sklar, Rudy Slingerland, and Kelin Whipple provided thoughtful and constructive reviews; Kelin Whipple also pointed us to some relevant manuscripts in press.

REFERENCES

Anderson, R.S., Evolution of the Santa Cruz Mountains, California, through tectonic growth and geomorphic decay, *J. Geophys. Res.*, *99*, 20161-20180, 1994.

Bagnold, R.A., Bed load transport by natural rivers, *Water Res. Res.*, *13*, 303-312, 1977.

Baldwin, J.A., K.X. Whipple, and G.E. Tucker, Controls on the timescale of post-orogenic decay of topography, in *Proc. Earth System Processes Meeting*, pp. 96, Geol. Soc. Am. - Geol. Soc. London, Edinburgh, Scotland, 2001 (abstract).

Beaumont, C., P. Fullsack, and J. Hamilton, Erosional control of active compressional orogens, in *Thrust Tectonics*, edited by K.R. McClay, pp. 1-18, Chapman & Hall, London, 1992.

Beaumont, C., H. Kooi, and S. Willett, Progress in coupled tectonic - surface process models with applications to rifted margins and collisional orogens, in *Geomorphology and Global Tectonics*, edited by M.A. Summerfield, pp. 29-56, Wiley, Chichester, 2000.

Bierman, P.R., and M. Caffee, Cosmogenic exposure and erosion history of Australian bedrock landforms, *Geol. Soc. Am. Bull.*, *114*, 787-803, 2002.

Bishop, P., Southeast Australian late Mesozoic and Cenozoic denudation rates: A test for late Tertiary increases in continental denudation, *Geology*, *13*, 479-482, 1985.

Bishop, P., Horizontal stability of the Australian continental drainage divide in south central New South Wales during the Cainozoic, *Austr. J. Earth Sci.*, *33*, 295-307, 1986.

Bishop, P., and R. Brown, Denudational isostatic rebound of intraplate highlands: The Lachlan River valley, Australia, *Earth Surf. Proc. Landforms*, *17*, 345-360, 1992.

Bishop, P., and G. Goldrick, Geomorphological evolution of the East Australian continental margin, in *Geomorphology and Global Tectonics*, edited by M.A. Summerfield, pp. 225-254, Wiley, Chichester, 2000.

Bishop, P., R.W. Young, and I. McDougall, Stream profile change and longterm landscape evolution: Early Miocene and modern rivers of the east Australian highland crest, central New South Wales, Australia, *J. Geol.*, *93*, 455-474, 1985.

Brocard, G., Origine, importance, variabilité spatio-temporelle et signature morphologique de l'incision fluviatile dans les Alpes Dauphinoises (SE France), Ph.D. thesis, Université Joseph Fourier, Grenoble, 2002.

Densmore, A.L., M.A. Ellis, and R.S. Anderson, Landsliding and the evolution of normal-fault-bounded mountains, *J. Geophys. Res.*, *103*, 15203-15219, 1998.

DeYoung, V.N., Modeling the Geomorphic Evolution of Western Kauai, Hawaii: A study of surface processes in a basaltic terrain, MSc. thesis, Dalhousie University, Halifax, 2000.

Finlayson, D.P., D.R. Montgomery, and B. Hallet, Spatial coincidence of rapid inferred erosion with young metamorphic massifs in the Himalayas, *Geology*, *30*, 219–222, 2002.

Gardner, T.W., Experimental study of knickpoint and longitudinal profile evolution in cohesive, homogeneous material, *Geol. Soc. Am. Bull.*, *94*, 664-672, 1983.

Gasparini, N.M., G.E. Tucker, and R.L. Bras, Downstream fining through selective particle sorting in an equilibrium drainage network, *Geology*, *27*, 1079–1082, 1999.

Goldrick, G., A one-person, one-instrument method for precision barometric altimetry, *Earth Surf. Proc. Landforms, 19,* 801-808, 1994.

Goldrick, G., Bedrock stream long profile form and evolution; A new framework with case studies from the Lachlan Catchment, N.S.W., PhD. thesis, Monash University, Clayton, Vic., 1999.

Goldrick, G., and P. Bishop, Differentiating the role of lithology and uplift in the steepening of bedrock river long profiles: An example from southeastern Australia, *J. Geol.*, *103*, 227-231, 1995.

Hancock, G.S., R.S. Anderson, and K.X. Whipple, Beyond power: Bedrock river incision process and form, in *Rivers over Rock: Fluvial Processes in Bedrock Channels*, edited by K.J. Tinkler, and E.E. Wohl, pp. 35-60, American Geophysical Union, 1998.

Hartshorn, K., N. Hovius, W.B. Dade, and R.L. Slingerland, Climate-drive bedrock incision in an active mountain belt, *Science*, *297*, 2036-2038, 2002.

Hay, W.W., Detrital sediment fluxes from continents to oceans, *Chem. Geol.*, *145*, 287-323, 1998.

Heimsath, A.M., J. Chappell, W.E. Dietrich, K. Nishiizumi, and R.C. Finkel, Soil production on a retreating escarpment in southeastern Australia, *Geology*, *28*, 787-790, 2000.

Hovius, N., Macro-scale processes of mountain belt erosion, in *Geomorphology and Global Tectonics*, edited by M.A. Summerfield, pp. 77-106, Wiley, Chichester, 1999.

Howard, A.D., Long profile development of bedrock channels: Interaction of weathering, mass wasting, bed erosion, and sediment transport, in *Rivers over Rock: Fluvial Processes in Bedrock Channels*, edited by K.J. Tinkler, and E.E. Wohl, pp. 297-319, American Geophysical Union, 1998.

Howard, A.D., W.E. Dietrich, and M.A. Seidl, Modeling fluvial erosion on regional to continental scales, *J. Geophys. Res.*, *99*, 13971-13986, 1994.

Hurtrez, J.-E., F. Lucazeau, J. Lavé, and J.-P. Avouac, Investigation of the relationships between basin morphology, tectonic uplift, and denudation from the study of an active fold belt in the Siwalik Hills, central Nepal, *J. Geophys. Res.*, *104*, 12779-12796, 1999.

Kirby, E., and K.X. Whipple, Quantifying differential rock-uplift rates via stream profile analysis, *Geology*, *29*, 415-418, 2001.

Kooi, H., and C. Beaumont, Escarpment evolution on high-elevation rifted margins; insights derived from a surface processes model that combines diffusion, advection and reaction, *J. Geophys. Res.*, *99*, 12191-12210, 1994.

Lambeck, K., H.W.S. McQueen, R. Stephenson, and D. Denham, The state of stress within the Australian continent, *Ann. Geophys.*, *2*, 723-742, 1984.

Lambeck, K., and R. Stephenson, The post-Paleozoic uplift history of south-eastern Australia, *Austr. J. Earth Sci.*, *33* , 253-270, 1986.

Lavé, J., and J.P. Avouac, Fluvial incision and tectonic uplift across the Himalayas of central Nepal, *J. Geophys. Res.*, *106*, 25561-25593, 2001.

Leopold, L.B., M.G. Wolman, and J.P. Miller, *Fluvial Processes in Geomorphology*, 522 pp., Freeman, New York, 1964.

Montgomery, D.R., T.B. Abbe, J.M. Buffington, N.P. Peterson, K.M. Schmidt, and J.D. Stock, Distribution of bedrock and alluvial channels in forested mountain drainage basins, *Nature, 381*, 587-589, 1996.

Pazzaglia, F.J., and M.T. Brandon, A fluvial record of long-term steady-state uplift and erosion across the Cascadia forearc high, western Washington State, *Am. J. Sci.*, *301*, 385-431, 2001.

Pazzaglia, F.J., T.W. Gardner, and D.J. Merritts, Bedrock fluvial incision and longitudinal profile development over geologic time scales determined by fluvial terraces, in *Rivers over Rock: Fluvial Processes in Bedrock Channels*, edited by K.J. Tinkler, and E.E. Wohl, pp. 207-235, American Geophysical Union, 1998.

Press, W.H., S.A. Teukolsky, W.T. Vetterling, and B.P. Flannery, *Numerical Recipes in Fortran 77; The Art of Scientific Computing*, 921 pp., Cambridge University Press, New York, 1992.

Roe, G.H., D.R. Montgomery, and B. Hallet, Effects of orographic precipitation variations on the concavity of steady-state river profiles, *Geology*, *30*, 143-146, 2002.

Royden, L.H., M.K. Clark, and K.X. Whipple, Evolution of river-elevation profiles by bedrock incision: Analytical solution to transient river profiles related to changing uplift and precipitation rates, *EOS Trans. AGU*, *81*(Fall Meeting Suppl), F 1142, 2000.

Seidl, M.A., and W.E. Dietrich, The problem of channel erosion into bedrock, in *Functional Geomorphology*, edited by K.-H. Schmidt, and J. de Ploey, *CATENA Suppl., 23,* 101-124, 1992.

Seidl, M.A., W.E. Dietrich, and J.W. Kirchner, Longitudinal profile development into bedrock: an analysis of Hawaiian channels, *J. Geol.*, *102*, 457-474, 1994.

Sklar, L., and W.E. Dietrich, River longitudinal profiles and bedrock incision models: Stream power and the influence of sediment supply, in *Rivers over Rock: Fluvial Processes in Bedrock Channels*, edited by K.J. Tinkler, and E.E. Wohl, pp. 237-260, American Geophysical Union, 1998.

Sklar, L., and W.E. Dietrich, Sediment and rock strength controls on river incision into bedrock, *Geology*, *29*, 1087-1090, 2001.

Slingerland, R., S.D. Willett, and H. Hennessey, A new fluvial bedrock erosion model based on the work-energy principle, *EOS Trans. AGU*, *78* (Fall Meeting Suppl.), 299, 1997.

Slingerland, R., S.D. Willett, and N. Hovius, Slope-area scaling as a test of fluvial incision laws, *EOS Trans. AGU*, *79* (Fall Meeting Suppl.), F358, 1998.

Snyder, N.P., K.X. Whipple, G.E. Tucker, and D.J. Merrits, Landscape response to tectonic forcing: Digital elevation model analysis of stream profiles in the Mendocino triple junction region, northern California, *Geol. Soc. Am. Bull.*, *112*, 1250-1263, 2000.

Snyder, N.P., K.X. Whipple, G.E. Tucker, and D.J. Merrits, The importance of a stochastic distribution of floods and erosion thresholds in the bedrock river incision problem, *J. Geophys. Res.*, *in press*, 2003.

Stock, J.D., and D.R. Montgomery, Geologic constraints on bedrock river incision using the stream power law, *J. Geophys. Res.*, *104*, 4983-4993, 1999.

Talling, P.J., and M.F. Sowter, Erosion, deposition and basin-wide variations in stream power and bed shear stress, *Basin Res.*, *10*, 87-108, 1998.

Tinkler, K.J., and E.E. Wohl, Editors: *Rivers Over Rock: Fluvial Processes in Bedrock Channels*, American Geophysical Union, 1998.

Tomkin, J.H., M.T. Brandon, F.J. Pazzaglia, J.R. Barbour, and S.D. Willett, Quantitative testing of bedrock incision models for the Clearwater River, NW Washington State, *J. Geophys. Res.*, *in press*, 2003.

Tucker, G.E., and R.L. Slingerland, Erosional dynamics, flexural isostasy, and long-lived escarpments: a numerical modeling study, *J. Geophys. Res.*, *99*, 12229-12243, 1994.

Tucker, G.E., and R.L. Slingerland, Drainage basin responses to climate change, *Wat. Resour. Res.*, *33*, 2031-2047, 1997.

Tucker, G.E., and K.X. Whipple, Topographic outcomes predicted by stream erosion models: sensitivity analysis and intermodel comparison, *J. Geophys. Res.*, *107*, 2179, doi: 10.1029/2001JB000162, 2002.

van der Beek, P.A., and J. Braun, Numerical modelling of landscape evolution on geological time-scales: A parameter analysis and comparison with the south-eastern highlands of Australia, *Basin Res.*, *10*, 49-68, 1998.

van der Beek, P.A., and J. Braun, Controls on post-mid-Cretaceous landscape evolution in the southeastern highlands of Australia: Insights from numerical surface process models, *J. Geophys. Res.*, *104*, 4945-4966, 1999.

van der Beek, P.A., J. Braun, and K. Lambeck, The post-Paleozoic uplift history of south-eastern Australia revisited: results from a process-based model of landscape evolution, *Austr. J. Earth Sci.*, *46*, 157-172, 1999.

Wellman, P., and I. McDougall, Potassium-argon ages on the Cainozoic volcanic rocks of New South Wales, *J. Geol. Soc. Australia*, *21*, 247-272, 1974.

Whipple, K.X., G.S. Hancock, and R.S. Anderson, River incision into bedrock: Mechanics and relative efficacy of plucking, abrasion, and cavitation, *Geol. Soc. Am. Bull.*, *112*, 490-503, 2000a.

Whipple, K.X., N.P. Snyder, and K. Dollenmayer, Rates and processes of bedrock incision by the Upper Ukak River since the 1912 Novarupta ash flow in the Valley of Ten Thousand Smokes, Alaska, *Geology, 28*, 835-838, 2000b.

Whipple, K.X., and G.E. Tucker, Dynamics of the stream-power river incision model: Implications for height limits of mountain ranges, landscape response timescales, and research needs, *J. Geophys. Res.*, *104*, 17661-17674, 1999.

Whipple, K.X., and G.E. Tucker, Implications of sediment-flux dependent river incision models for landscape evolution, *J. Geophys. Res.*, *107*, 2039, doi: 10.1029/2000JB000044, 2002.

Willett, S.D., Orogeny and orography: The effects of erosion on the structure of mountain belts, *J. Geophys. Res.*, *104*, 28957-28981, 1999.

Willgoose, G.R., R.L. Bras, and I. Rodriguez-Iturbe, A physically based coupled network growth and hillslope evolution model, 1, theory, *Water Res. Res.*, *27*, 1671-1684, 1991.

FIGURE CAPTIONS

Figure 1. Digital elevation model of the Upper Lachlan catchment, based on 9 arc-second AUSLIG topography data, showing drainage net and catchment boundaries extracted from the data, as well as main localities referred to in the text. Cross labeled 'B' indicates location of Boorowa Basalt at the Boorowa-Lachlan confluence. Box indicates extent of Figure 2; inset shows location within Southeastern Australia. Dotted line is the continental drainage divide; continuous line is the seaward-facing escarpment.

Figure 2. Detailed map of study area, showing basalt remnants (dark shading), bedrock geology (light shading: Paleozoic metamorphic rocks of the Adaminaby Group; white: Late Paleozoic Wyangala Granite; thick dashed line: hornfels ridge), elevations of basalt tops used for stream profile reconstruction (annotated crosses) and modeled streams (thick black lines). Profile line shows location of Figure 3. Australian Map Grid Reference (AMG) coordinates.

Figure 3. Cross-section across the middle reaches of Lampton and Merrill Creeks, showing the spatial relationships between the basalt top, sub-basaltic surface, and present-day beds of 'twin-lateral' streams. Dotted lines show reconstructed topography at time of basalt eruption; note initial concave upper surface of basalt flow and incision of twin-lateral streams at edge of flow. Best possible estimate of post-basalt fluvial incision is shown by double arrow. Elevation is from the Gunning 1:50,000 topographic map sheet; sub-basaltic surface from *Bishop et al.* [1985]

Figure 4. Relationships between present-day river profile, fluvial terraces, 12.5 Ma Boorowa basalt, and alluvial fill at the bedrock-alluvial transition along the Lachlan River close to Cowra. Modified from *Bishop and Brown* [1992] and *Goldrick* [1999].

Figure 5. Present-day river profiles for Lachlan River / Humes Creek, Merrill Creek, Lampton / Biala Creek and Wheeo Creek / Crookwell River, with projected elevations of tops of basalt remnants. Sub-basaltic surface is from *Bishop et al.* [1985]. See text for discussion on how 'probable' and 'possible' maximum elevations of supra-basaltic surface were constructed.

Figure 6. Relationships between (a) distance and contributing drainage area; (b) drainage area and stream width; (c) distance and local river slope (DS plot); and (d) drainage area and slope for the Lachlan River and Wheeo, Merrill and Lampton Creeks. Best-fit power laws are given for distance-area and area-width plots. In (d), the grey line shows the critical slope-area for the bedrock-alluvial transition suggested by *Montgomery et al.* [1996].

Figure 7. Present-day fluvial profiles for the Lachlan River and Wheeo, Lampton and Merrill Creeks predicted by the Detachment-Limited Stream Power model for different values of K, m, and n. Light and dark shaded lines indicate observed initial and present-day profiles, respectively.

Figure 8. Plots of misfit (modeled – observed incision) as a function of distance downstream for the models shown in Figure 7. Dashed line is best-fit linear regression of the points; its slope represents the misfit structure (s).

Figure 9. Contour plots of weighted mean RMS Misfit and Misfit structure for the Stream Power incision models. (a) Results for Detachment-Limited Stream Power model (equation 1), as a function of m and n. (b) Results for Transport-Limited Stream Power model (equations 4, 5), as a function of m_t and n_t.

Figure 10. (a) Results of Monte Carlo sampling of the parameter space for the Excess Stream Power model (equation 3): the panels show RMS Misfit as a function of m, n, normalized K (= K / $K^*_{(m,n)}$ as defined in equation 12) and C_0, respectively. The plots show 448 results out of 528 test, other models have mean RMS Misfits > 160 m. (b) Contour plots of weighted mean RMS Misfit as a function of K and C_0, for two m, n combinations: Left panel: $m = 0.4$, $n = 1$; right panel: $m = 0.3$, $n = 0.7$.

Figure 11. Present-day fluvial profiles for the Lachlan River and Wheeo, Lampton and Merrill Creeks predicted by the Tranport-Limited Stream Power model for different values of K_t, m_t, and n_t. Light and dark shaded lines indicate observed initial and present-day profiles, respectively.

Figure 12. Plots of RMS Misfit and Misfit structure for the Linear Undercapacity models (equations (4) and (7) with $m_t = n_t = 1$), as a function of K_t and L_f. (a) Constant width model, in which $W = 50$ m; (b) Variable width model, in which W varies as a function of A (equation 10).

Figure 13. Predicted present-day fluvial profiles for the Lachlan River and Wheeo, Lampton and Merrill Creeks predicted by the Undercapacity model for different values of K_t, L_f, m_t, and n_t. Light and dark shaded lines indicate observed initial and present-day profiles, respectively.

Figure 14. Results of Monte Carlo sampling of the parameter space for the Undercapacity model. Normalized $K_t = K_t / K^*_{t(L_f, m_t, n_t)}$ as defined in equation (13).

Figure 15. (a) Plots of RMS Misfit for the Linear Tools model (equations (4) and (8) with $m_t = n_t = 1$), as a function of K_t and L_f. Left plot is for a constant width ($W = 50$ m) model; right plot for a variable-width model in which W varies with A as in equation (10). (b) Results of Monte Carlo sampling of the parameter space for the Tools model. Normalized $K_t = K_t / K^*_{t(L_f, m_t, n_t)}$ as defined in equation (13).

Figure 16. Plots of RMS misfit for individual streams. RMS misfit is plotted as a function of K for the Detachment-Limited Stream Power model with $m = 0.4$, $n = 1$ (upper panels), and as a function of K_t (middle panels) and L_f (lower panels) for the Linear Undercapacity model. To avoid clutter, predicted misfits are plotted for the Lachlan River and Wheeo Creek only, Lampton and Merrill Creek misfits generally follow that of the Lachlan River. Left panels show results using the probable maximum supra-basaltic surface (SBS) as the initial profile; right panels are for the possible maximum SBS as an initial profile.

Figure 17. Present-day fluvial profiles for the Lachlan River and Wheeo, Lampton and Merrill Creeks predicted by a Detachment-Limited Stream Power model ($m = 0.4$, $n = 1$) and a Linear Undercapacity model, both including variable lithologies. Boxes at bases of profiles identify lithologies over which stream reaches flow; shading:

Adaminaby Group metamorphics ($K = 10^{-6}$ $m^{0.2}$ y^{-1} in Stream Power model, $L_f = 20$ km in Undercapacity model); white: Wyangala Granite ($K = 3\times10^{-7}$ $m^{0.2}$ y^{-1} in Stream Power model, $L_f = 100$ km in Undercapacity model).

Figure 18. Predicted present-day sediment flux and equilibrium carrying capacity for different Linear Undercapacity models. See text for discussion.

Table 1. RMS Misfit and Misfit Structure predicted by the best-fit parameter combinations for different fluvial incision models; Predicted river profiles for these models are shown in Figures 7, 11, 13 and 17.

Incision law / Best-fit parameters	Lachlan misfit (m)	Wheeo misfit (m)	Lampton misfit (m)	Merrill misfit (m)	Weighted Mean misfit (m)	Misfit structure (m km^{-1})
Detachment-Limited Stream Power						
$m = n = 1$; $K = 2.0\times10^{-12}$ m^{-1} y^{-1}	96	51	98	107	80	1.36
$m = 0.4$; $n = 1$; $K = 4.7\times10^{-7}$ $m^{0.2}$ y^{-1}	60	43	56	67	53	-0.09
$m = 0.4$; $n = 0.7$; $K = 9.0\times10^{-8}$ $m^{0.2}$ y^{-1}	56	24	62	71	45	0.30
$m = 0.3$; $n = 0.7$; $K = 7.0\times10^{-7}$ $m^{0.4}$ y^{-1}	51	26	50	60	42	-0.12
Excess Stream Power						
$m = 0.3$; $n = 0.7$; $K = 10^{-6}$ $m^{0.4}$ y^{-1}; $C_0 = 1.5\times10^{-6}$ m y^{-1}	52	53	41	58	52	0.18
$m = 0.4$; $n = 1$; $K = 8\times10^{-7}$ $m^{0.2}$ y^{-1}; $C_0 = 5\times10^{-7}$ m y^{-1}	51	98	34	46	67	0.19
Transport-Limited Stream Power						
$m_t = n_t = 1$; $K_t = 3.5\times10^{-6}$ m y^{-1}	83	51	67	76	68	-1.19
$m_t = 1.2$; $n_t = 0.7$; $K_t = 1.5\times10^{-8}$ $m^{0.6}$ y^{-1}	48	52	36	30	47	0.04
$m_t = 0.3$; $n_t = 0.7$; $K_t = 10$ $m^{2.4}$ y^{-1}	58	103	36	53	73	-0.63

Table 1. (Continued)

Incision law / Best-fit parameters	Lachlan misfit (m)	Wheeo misfit (m)	Lampton misfit (m)	Merrill misfit (m)	Weighted Mean misfit (m)	Misfit structure (m km^{-1})
Undercapacity						
Linear; $K_t = 10^{-5}$ m y^{-1}; $L_f = 1$ km; W = 50 m	36	84	21	44	54	0.25
Linear; $K_t = 10^{-5}$ m y^{-1}; $L_f = 30$ km; W = 50 m	66	60	79	93	67	0.67
Linear; $K_t = 10^{-5}$ m y^{-1}; $L_f = 30$ km; W = $f(A)$	53	62	40	58	55	-0.03
$m = 0.8$; $n = 0.4$; $K_t = 2.6\times10^{-5}$ m$^{1.4}$ y^{-1}; $L_f = 50$ km ; W = $f(A)$	30	51	32	45	38	0.22
Tools						
Linear; $K_t = 7\times10^{-6}$ m y^{-1}; $L_f = 3$ km; W = $f(A)$	57	82	75	65	69	0.62
$m = 1.1$; $n = 0.3$; $K_t = 2.6\times10^{-5}$ m$^{0.8}$ y^{-1}; $L_f = 1$ km ; W = $f(A)$	40	40	60	45	42	-0.02
Initial profile: Possible maximum SBS						
Stream Power: $m = 0.4$; $n = 1$; $K = 6\times10^{-7}$ m$^{0.2}$ y^{-1}	73	57	62	76	66	0.10
Undercapacity: $K_t = 1.5\times10^{-5}$ m y^{-1}; $L_f = 30$ km	45	101	47	28	65	-0.02
Two-lithology models						
Stream Power: $m = 0.4$; $n = 1$; $K = 3\text{-}10\times10^{-7}$ m$^{0.2}$ y^{-1}	47	19	50	34	35	0.18
Undercapacity: $K_t = 1.5\times10^{-5}$ m y^{-1}; $L_f = 20\text{-}100$ km	39	40	56	35	41	0.19

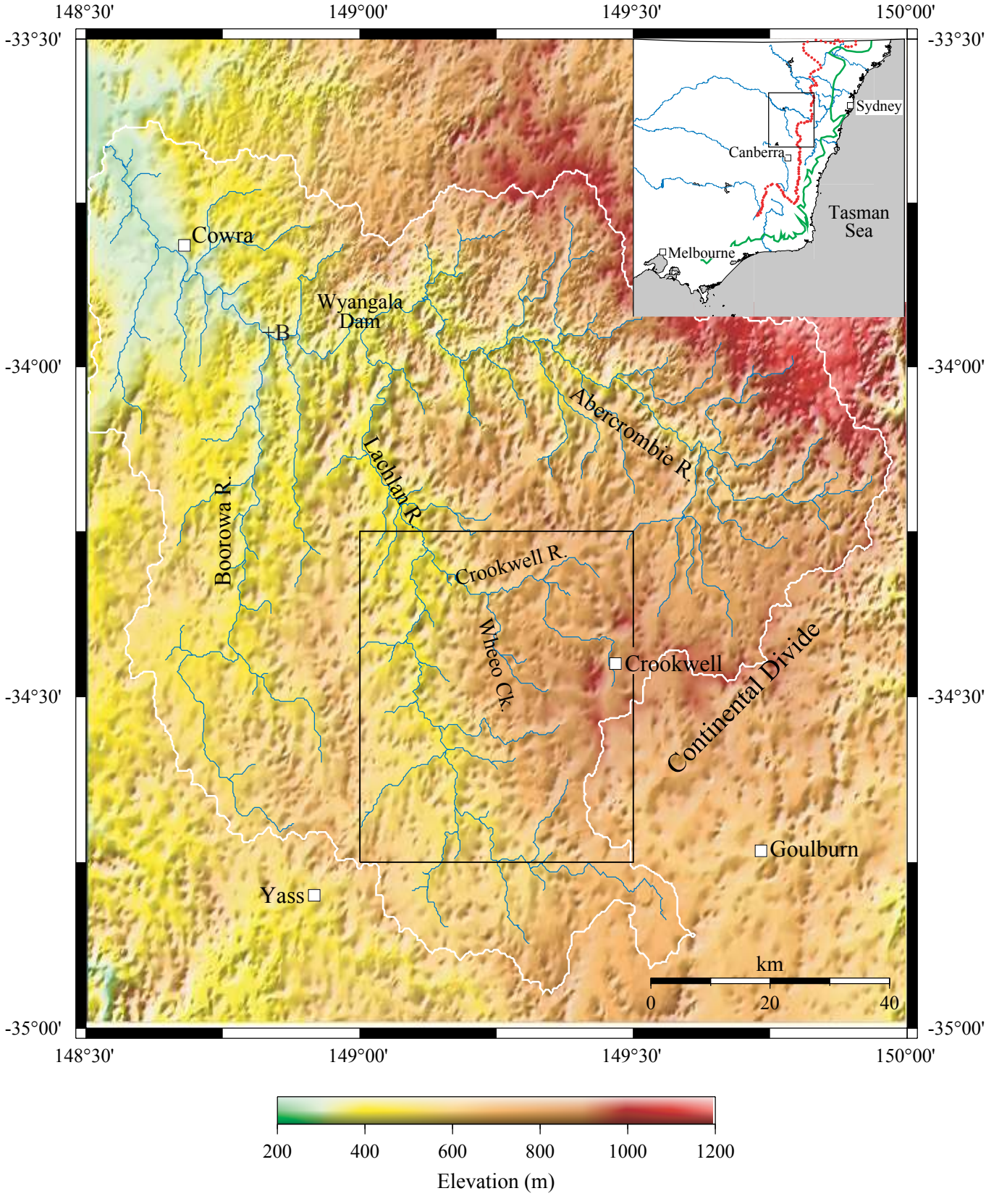

van der Beek and Bishop
Figure 1

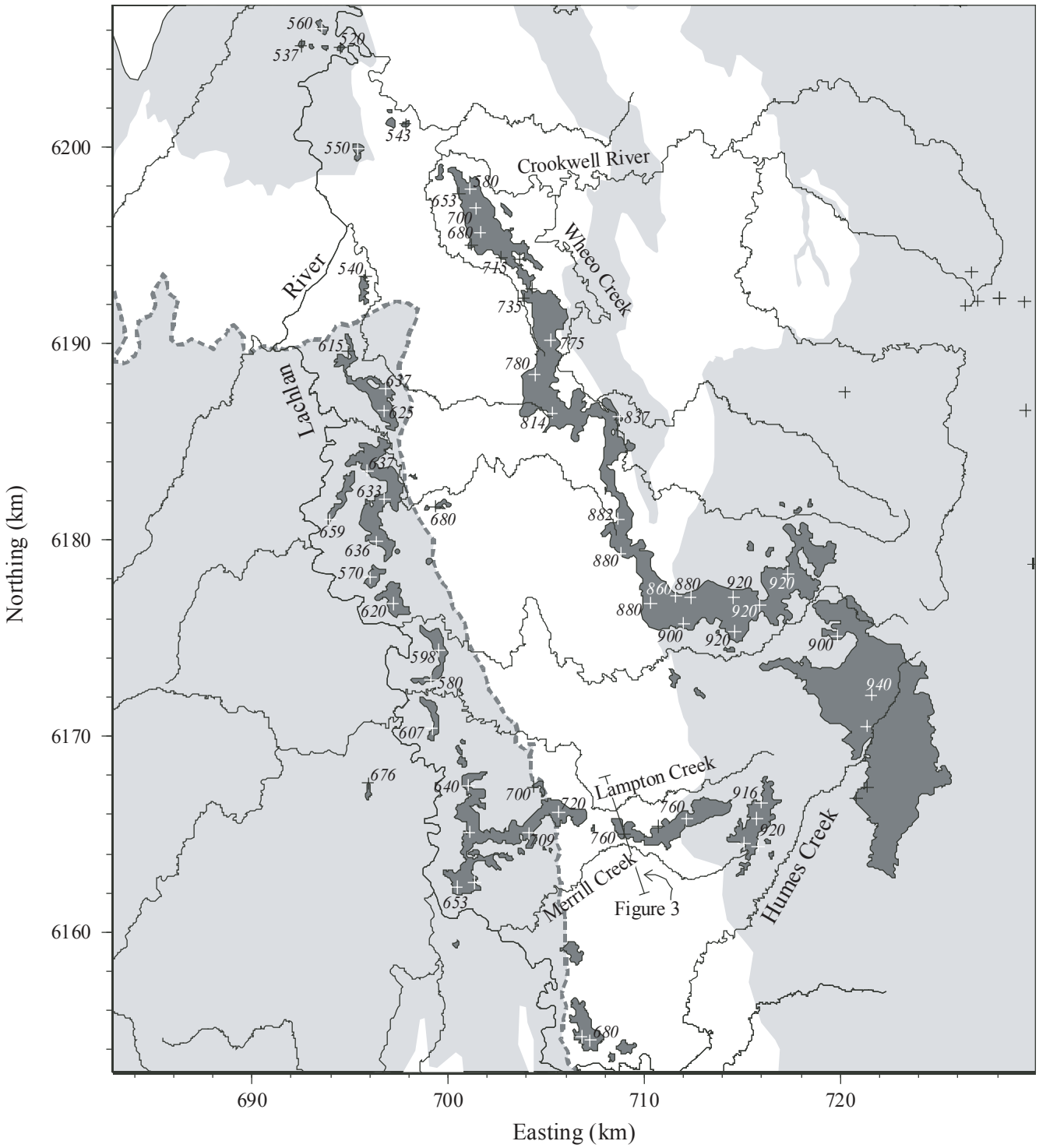

van der Beek and Bishop
Figure 2

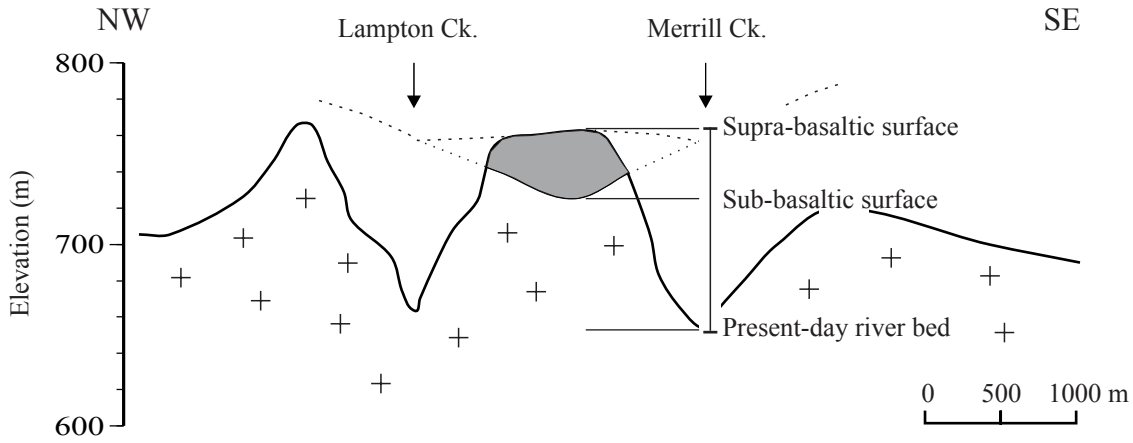

van der Beek and Bishop
Figure 3

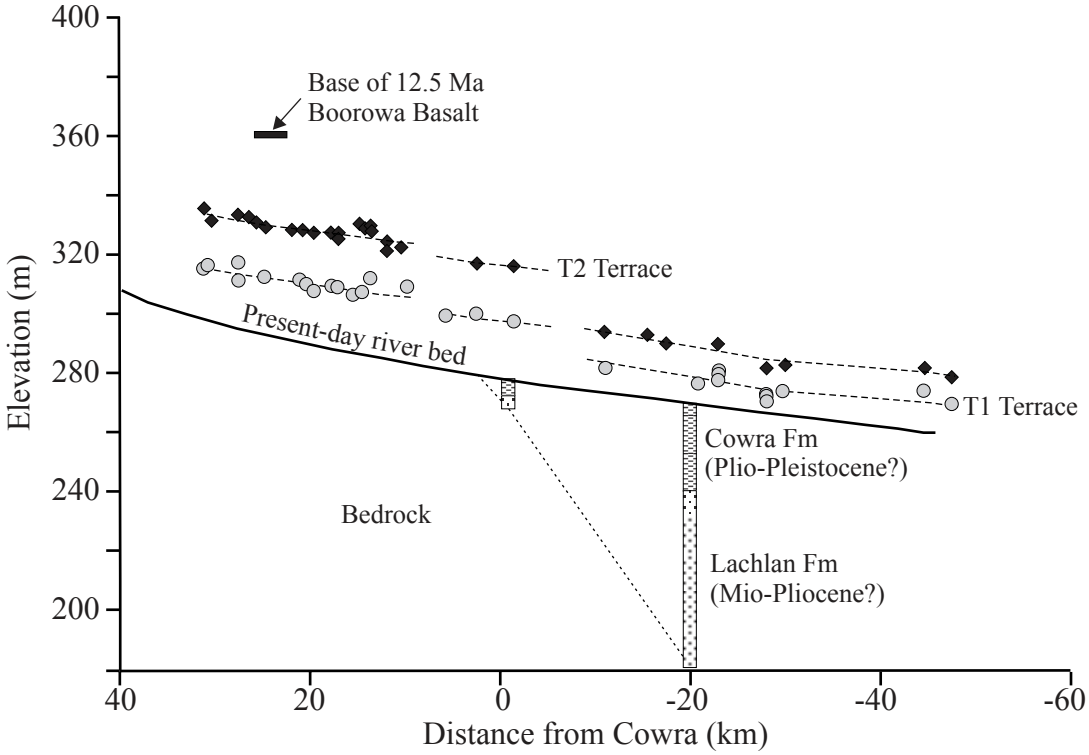

Van der Beek and Bishop
Figure 4

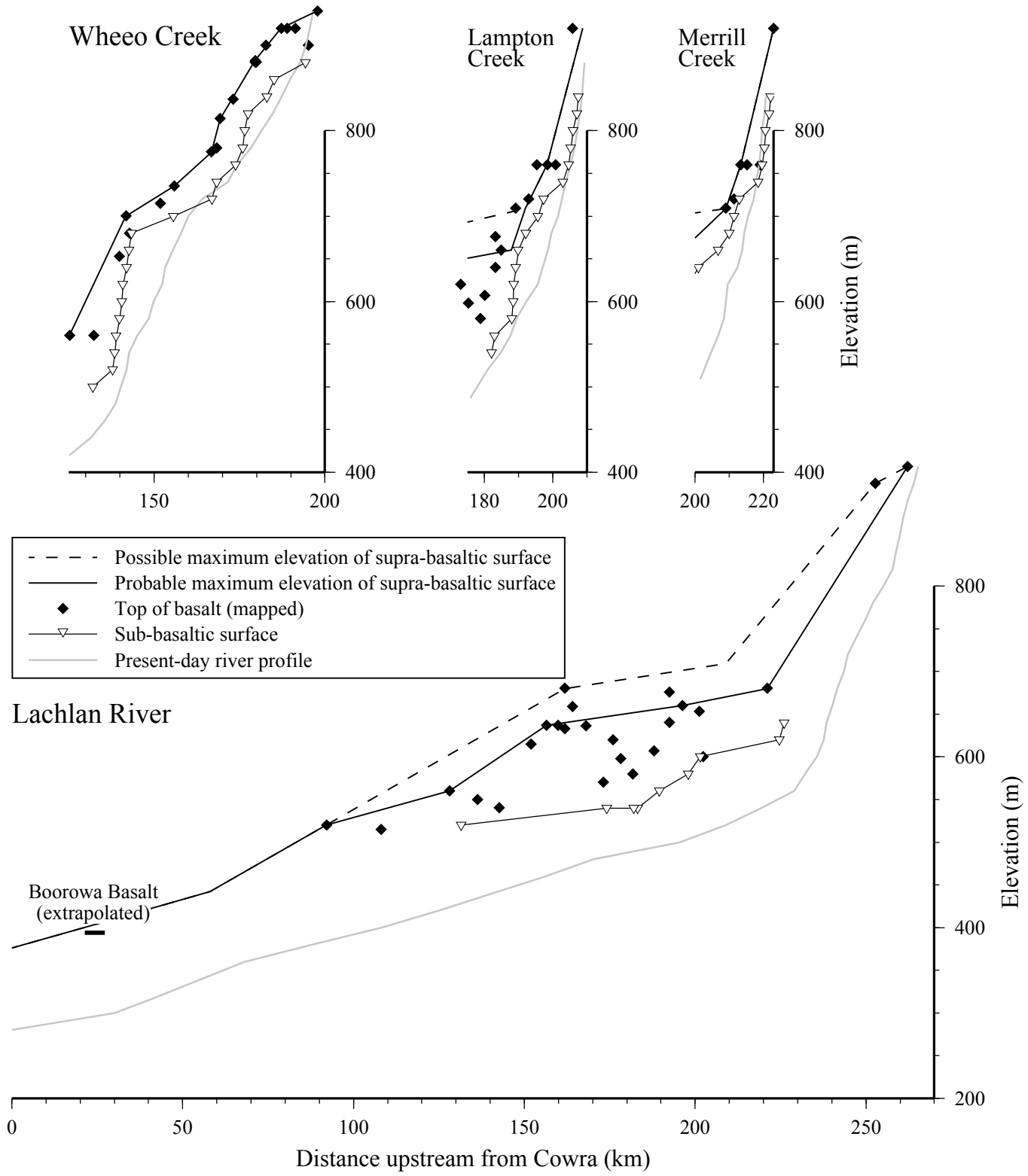

van der Beek and Bishop
Figure 5

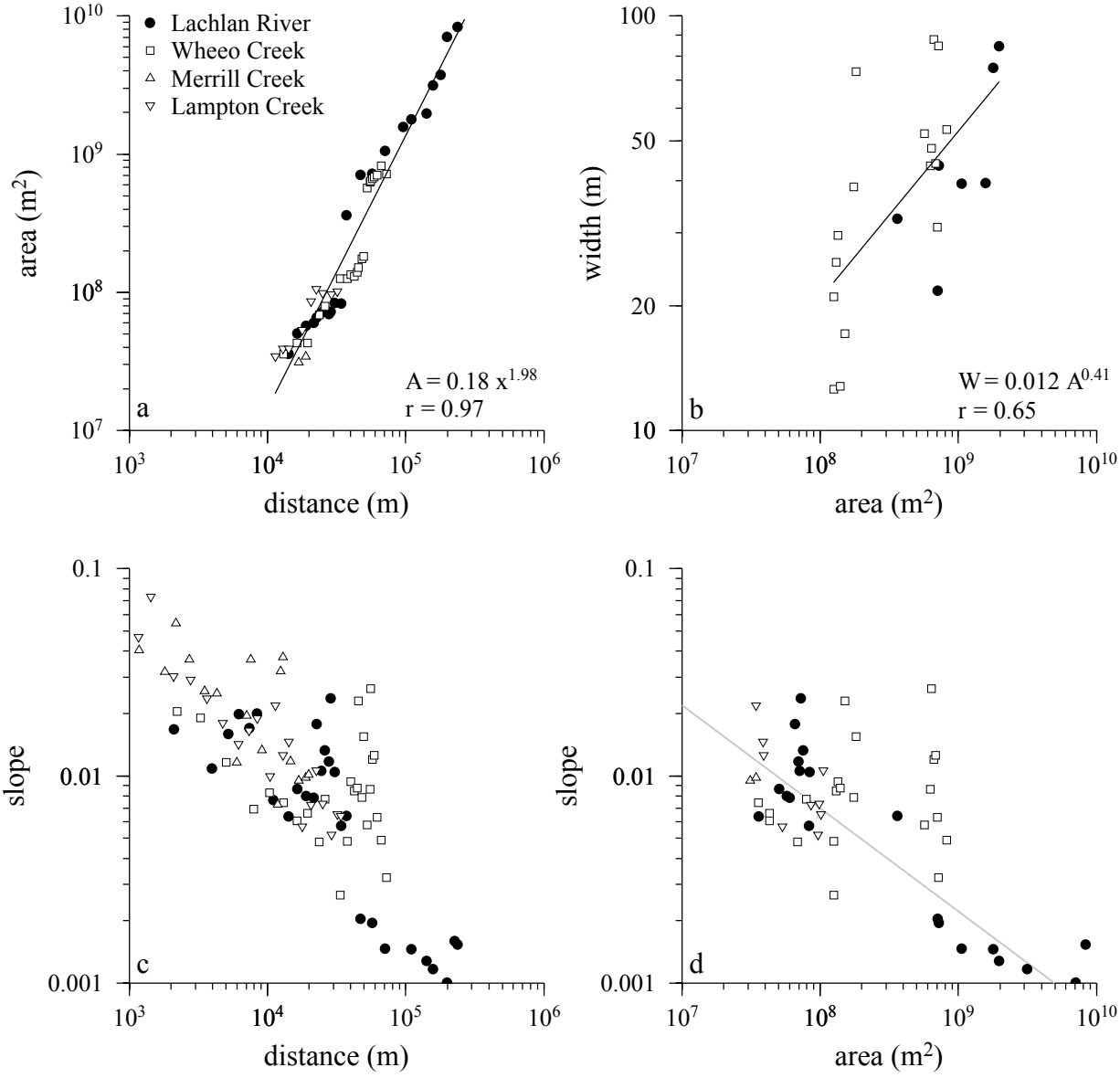

van der Beek and Bishop
Figure 6

Detachment-Limited Stream Power Models

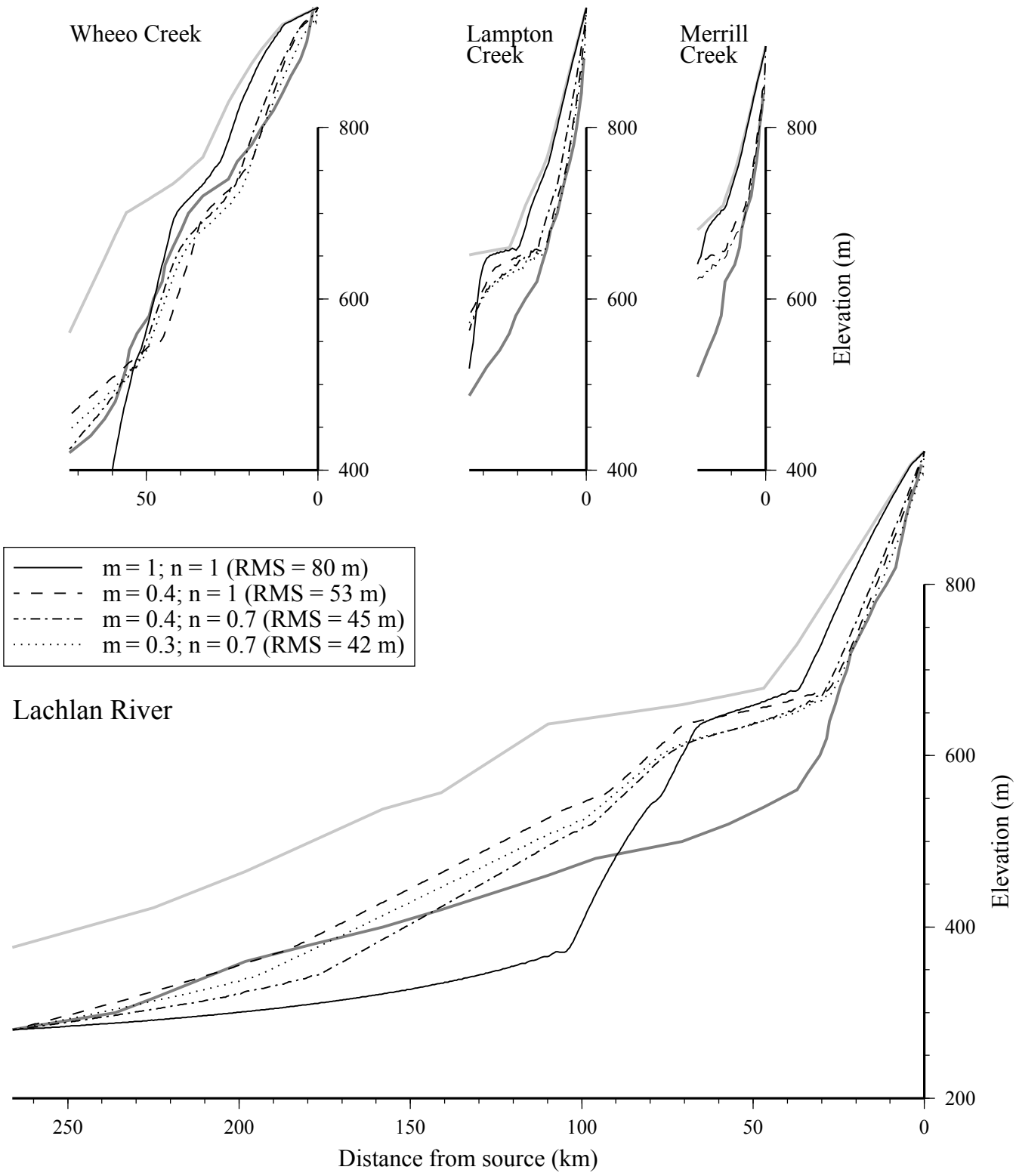

van der Beek and Bishop

Figure 7

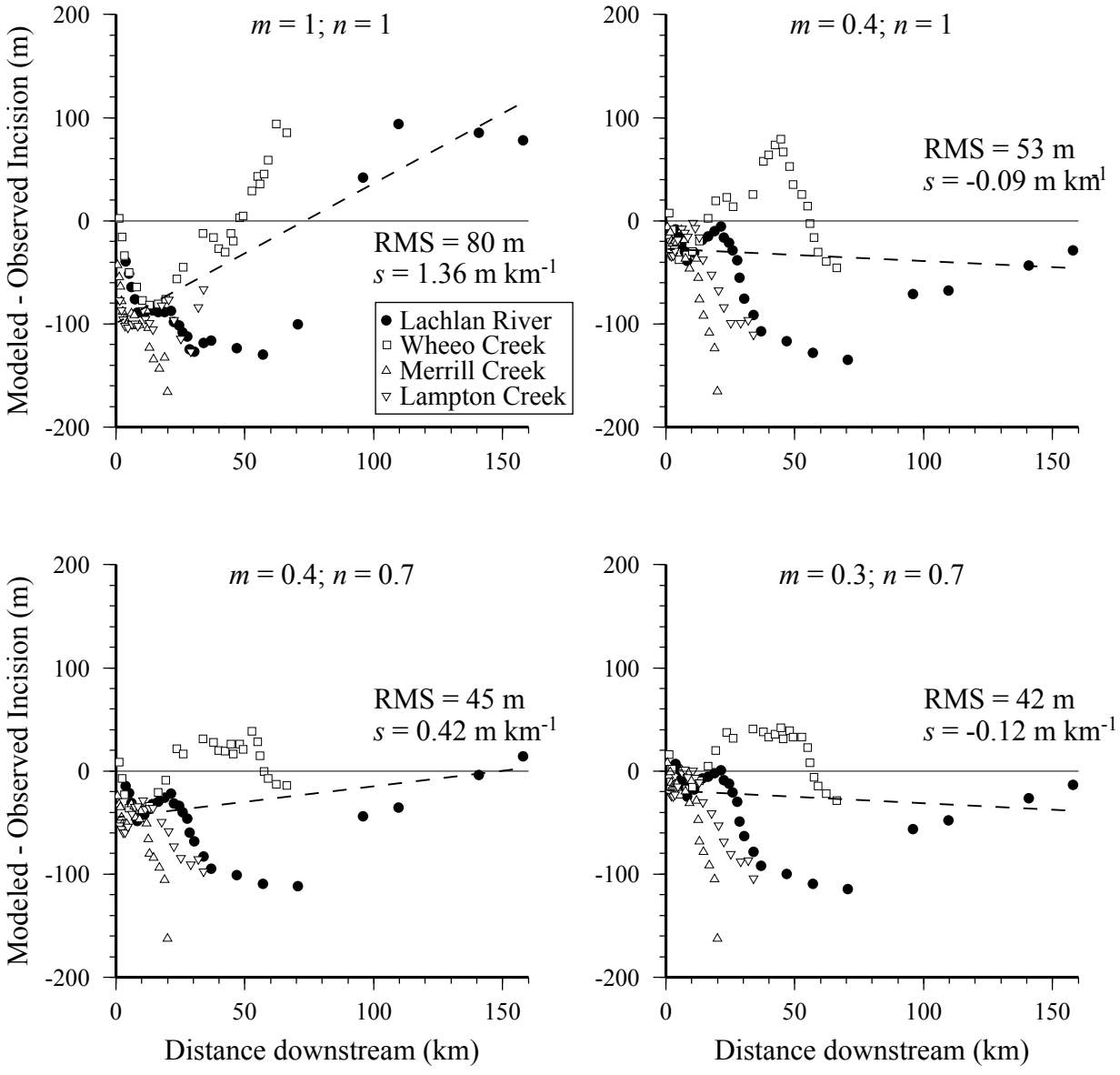

van der Beek and Bishop
Figure 8

a) Detachment-Limited Stream Power Model

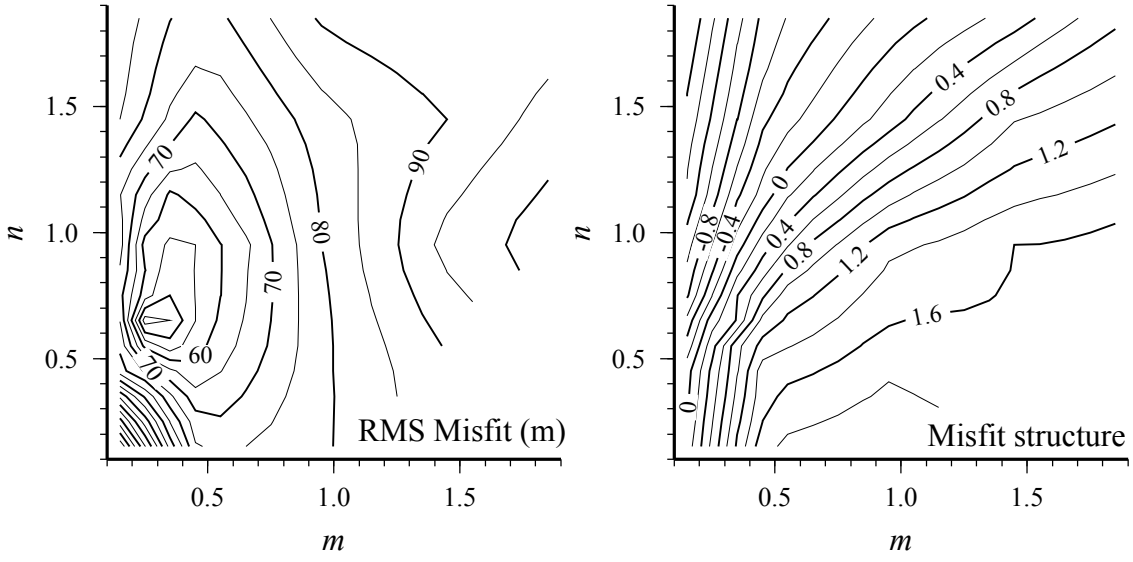

b) Transport-Limited Stream Power Model

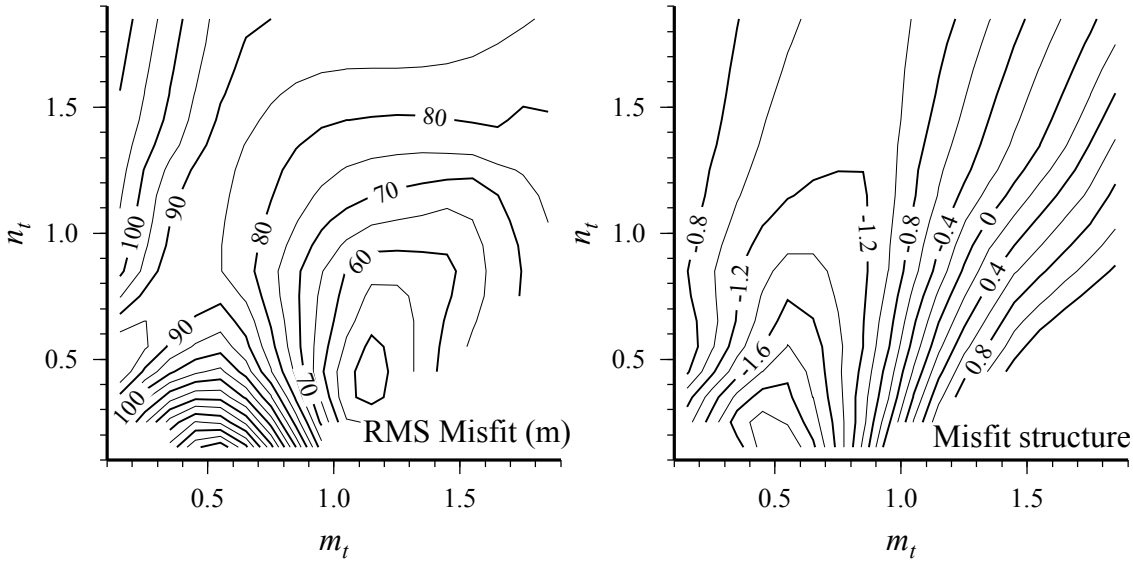

Excess Stream Power model

a) Monte Carlo results

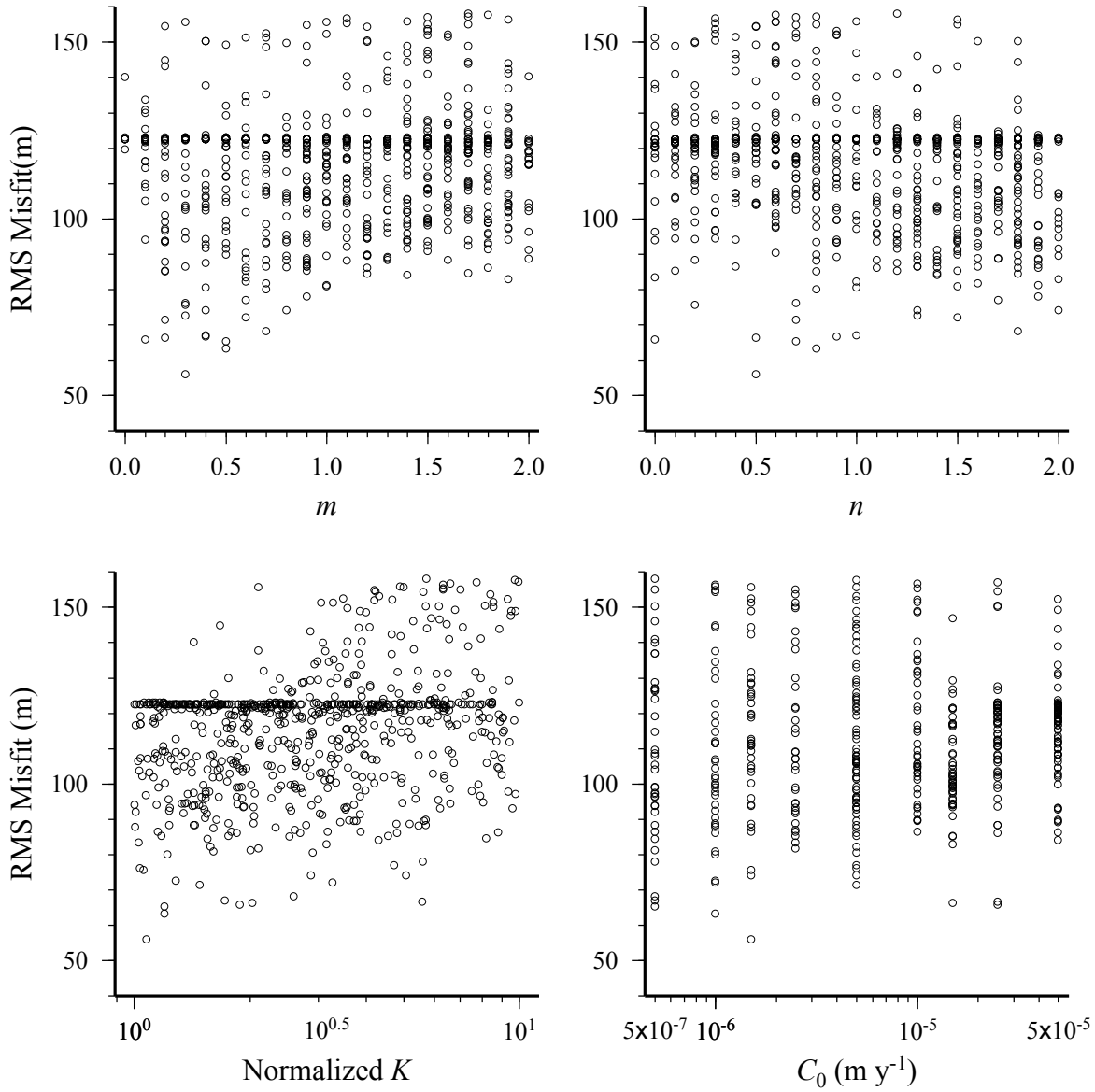

b) Systematic search results

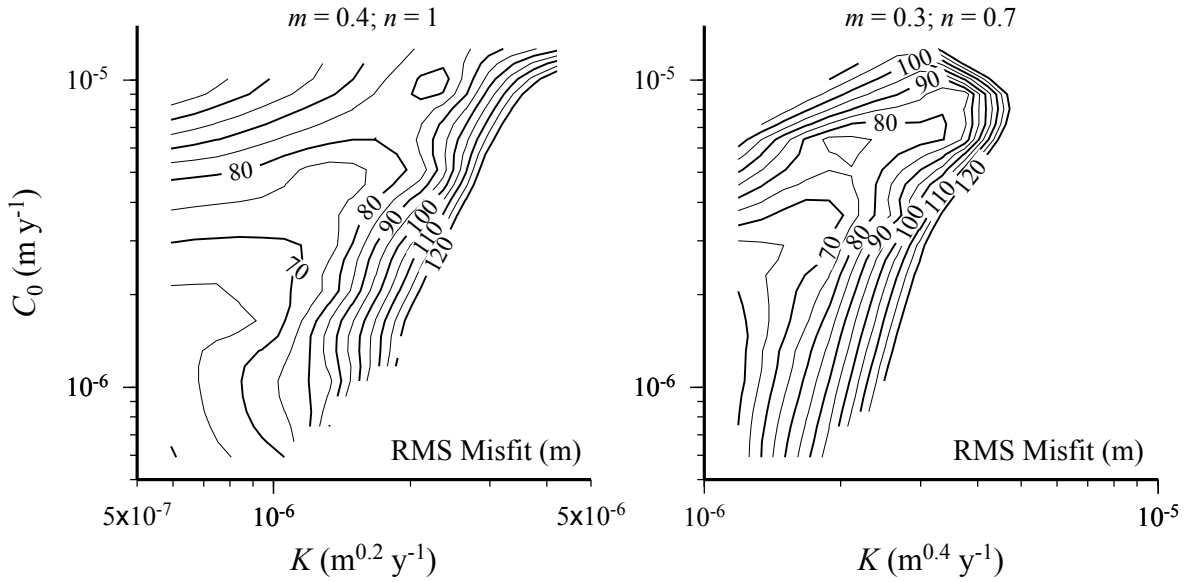

van der Beek and Bishop
Figure 10

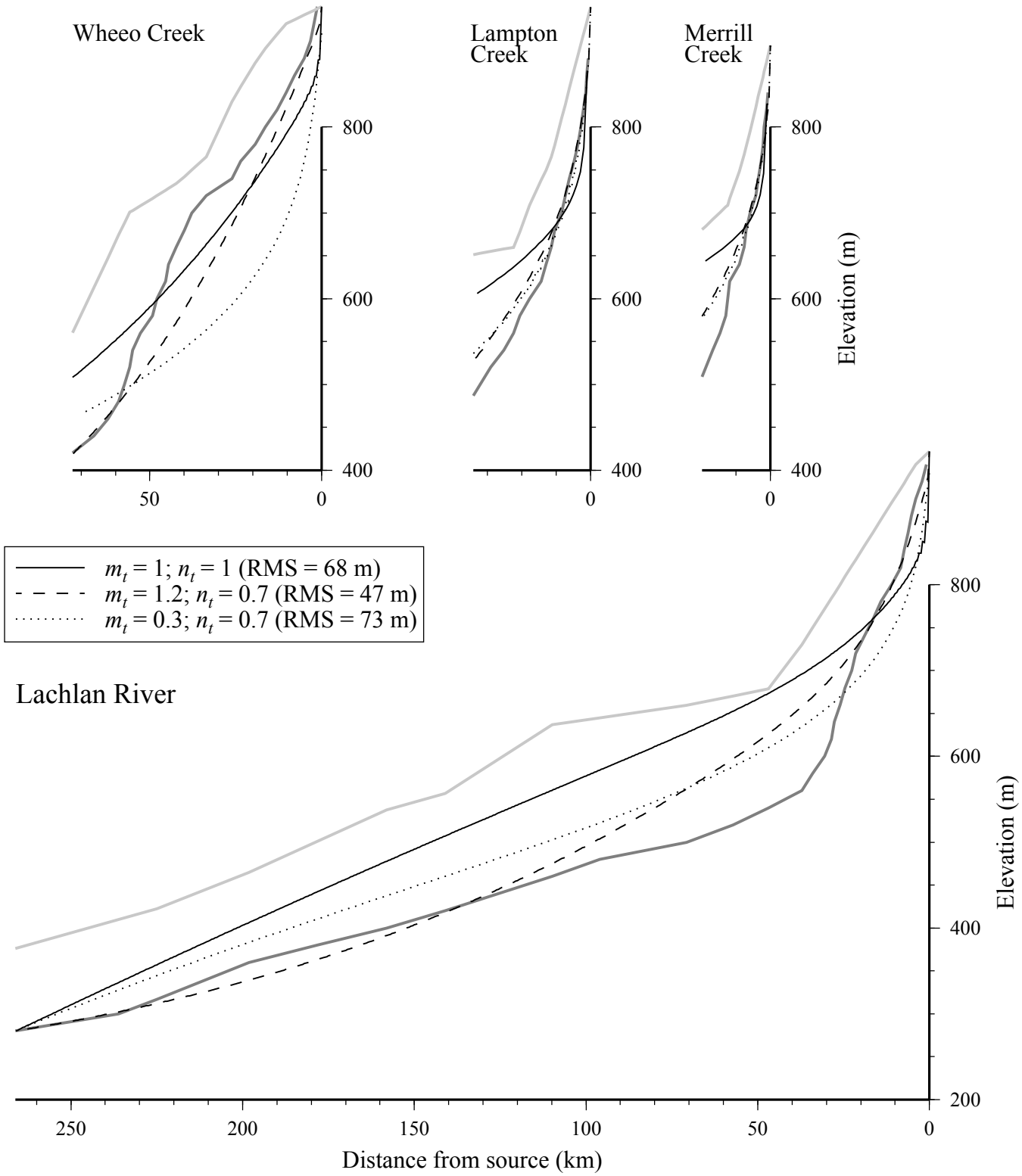

van der Beek and Bishop

Figure 11

a) Linear Undercapacity model; Constant Width

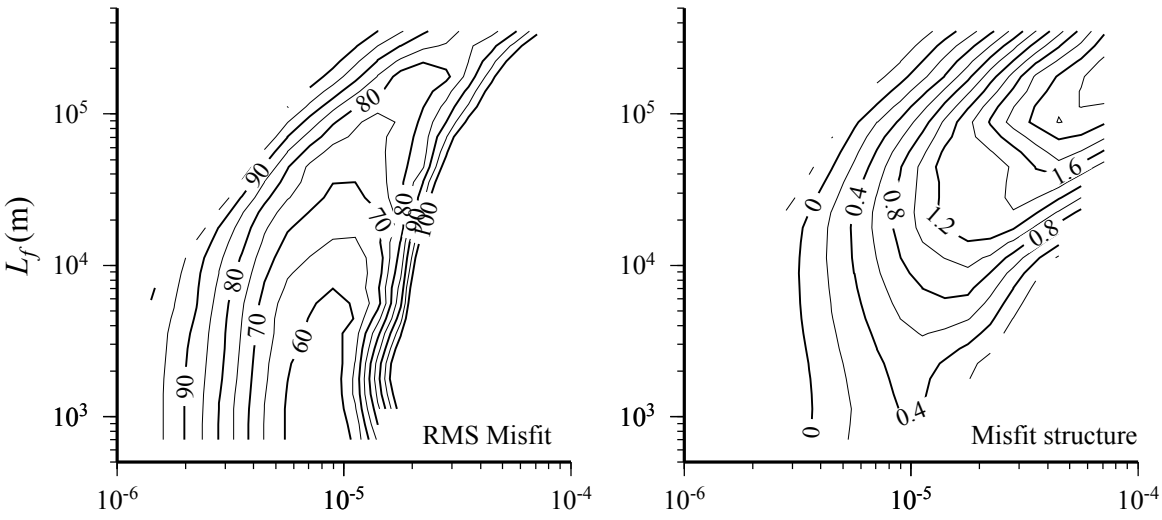

b) Linear Undercapacity model; Variable Width

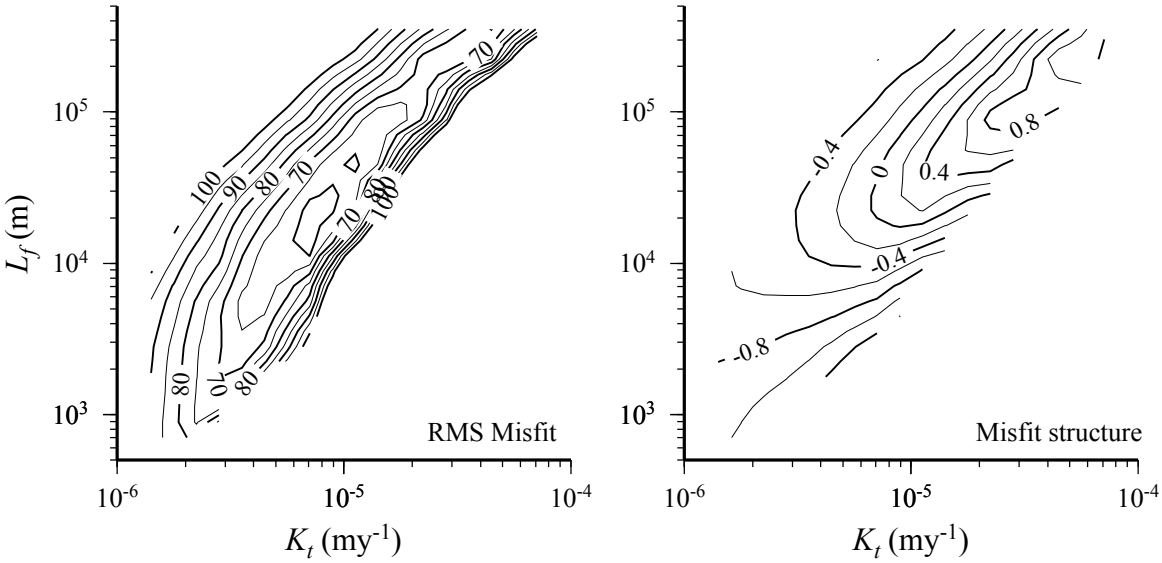

van der Beek and Bishop
Figure 12

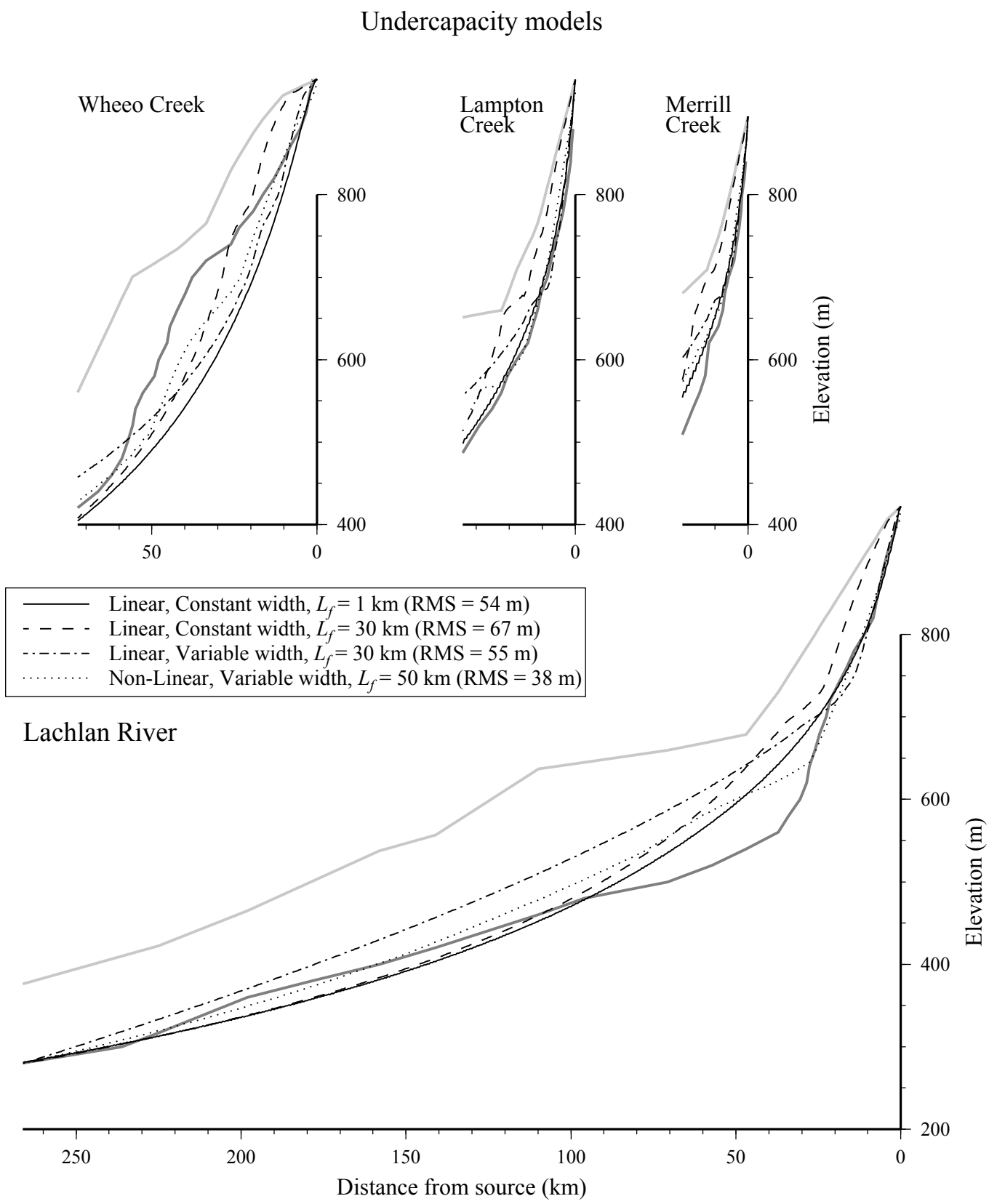

van der Beek and Bishop

Figure 13

Undercapacity model; Monte Carlo results

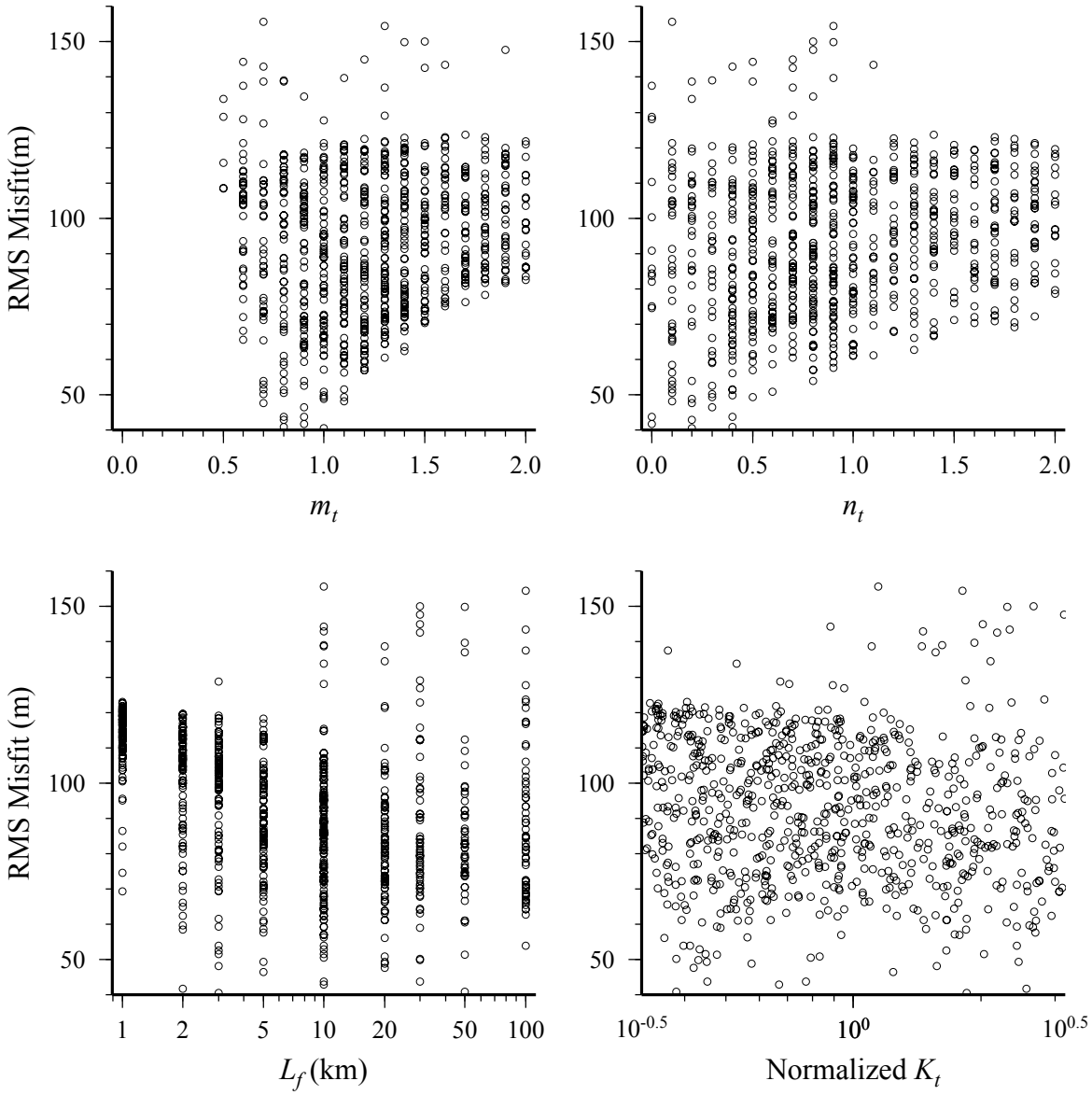

van der Beek and Bishop
Figure 14

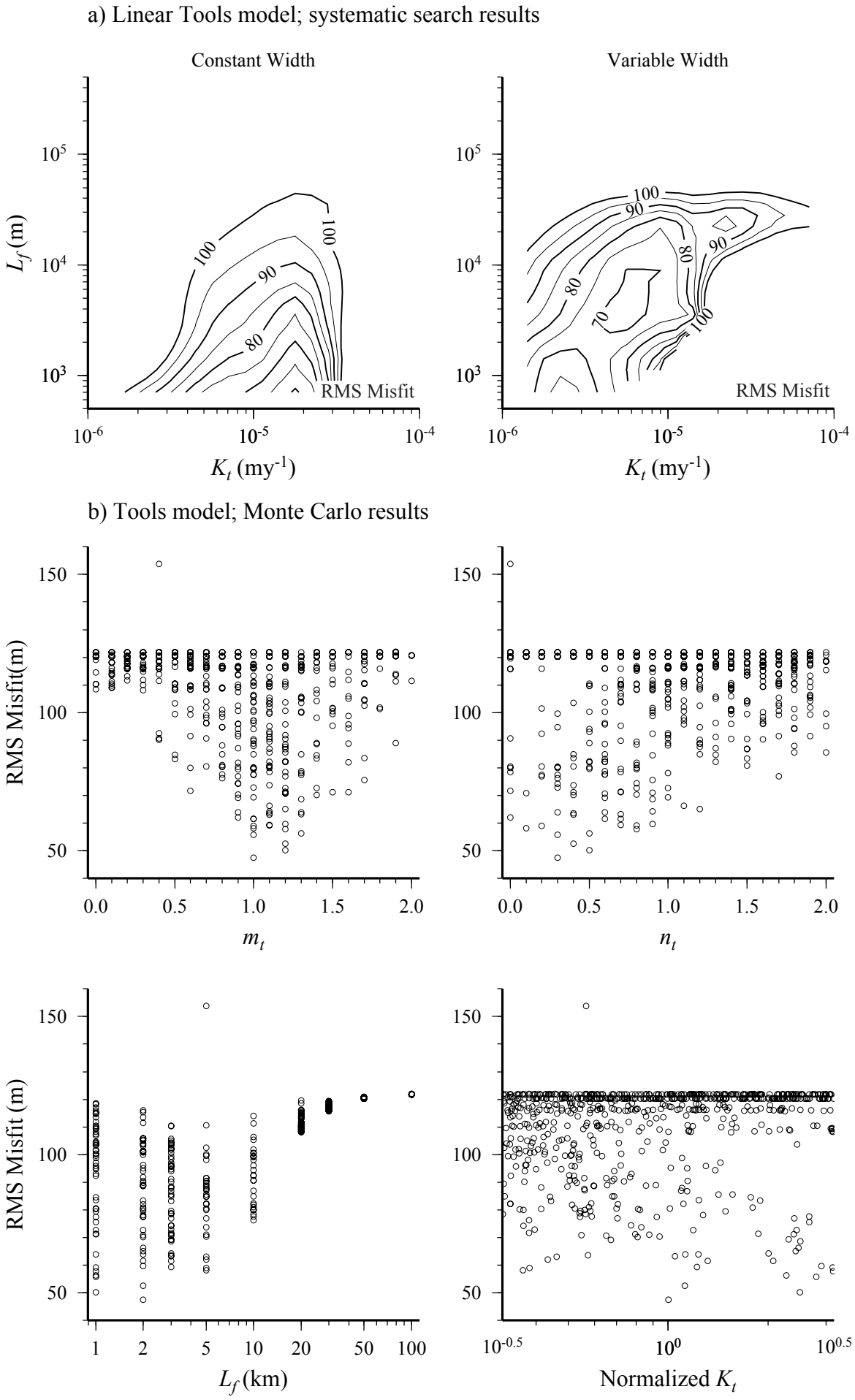

van der Beek and Bishop
Figure 15

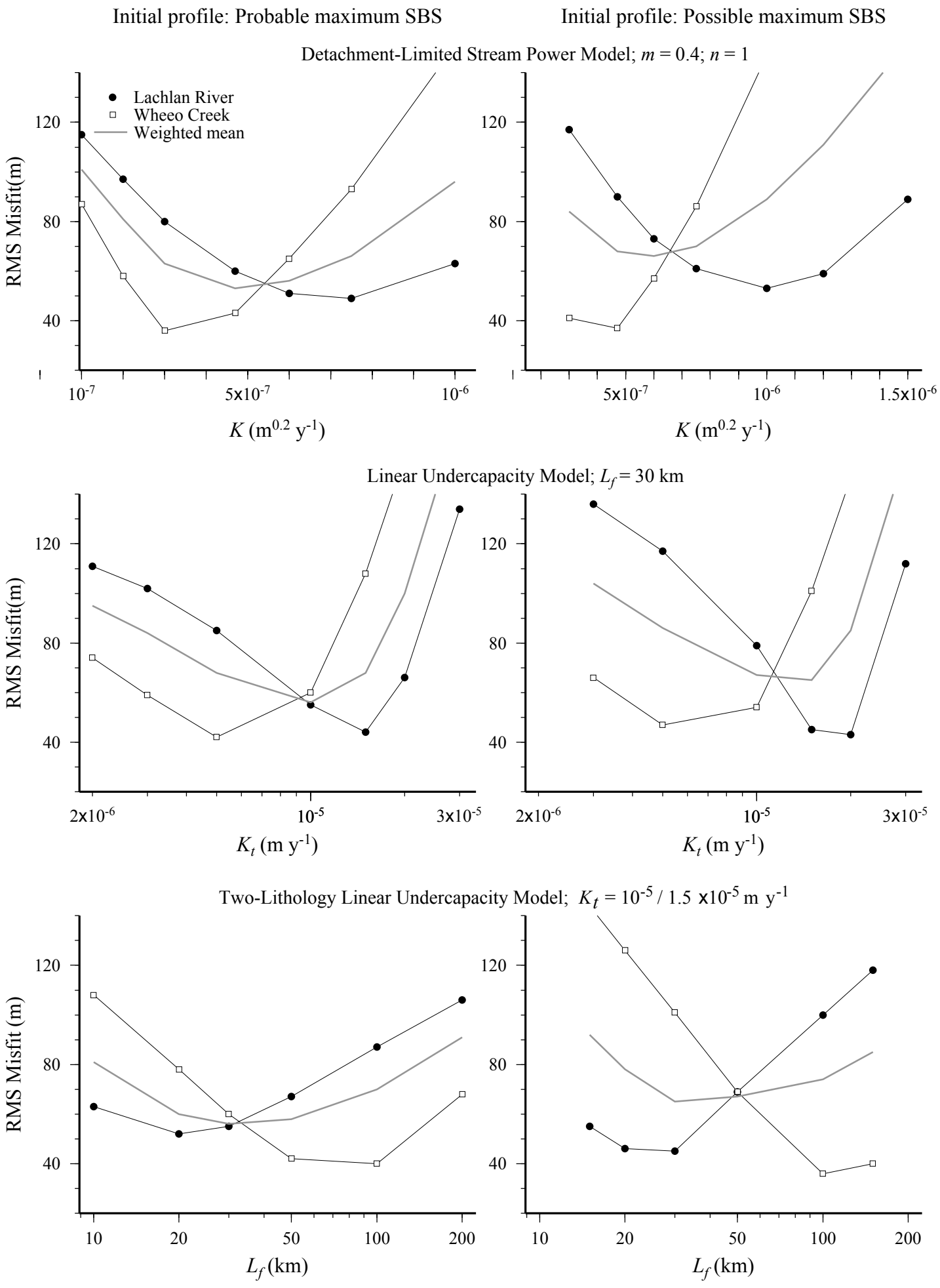

van der Beek and Bishop
Figure 16

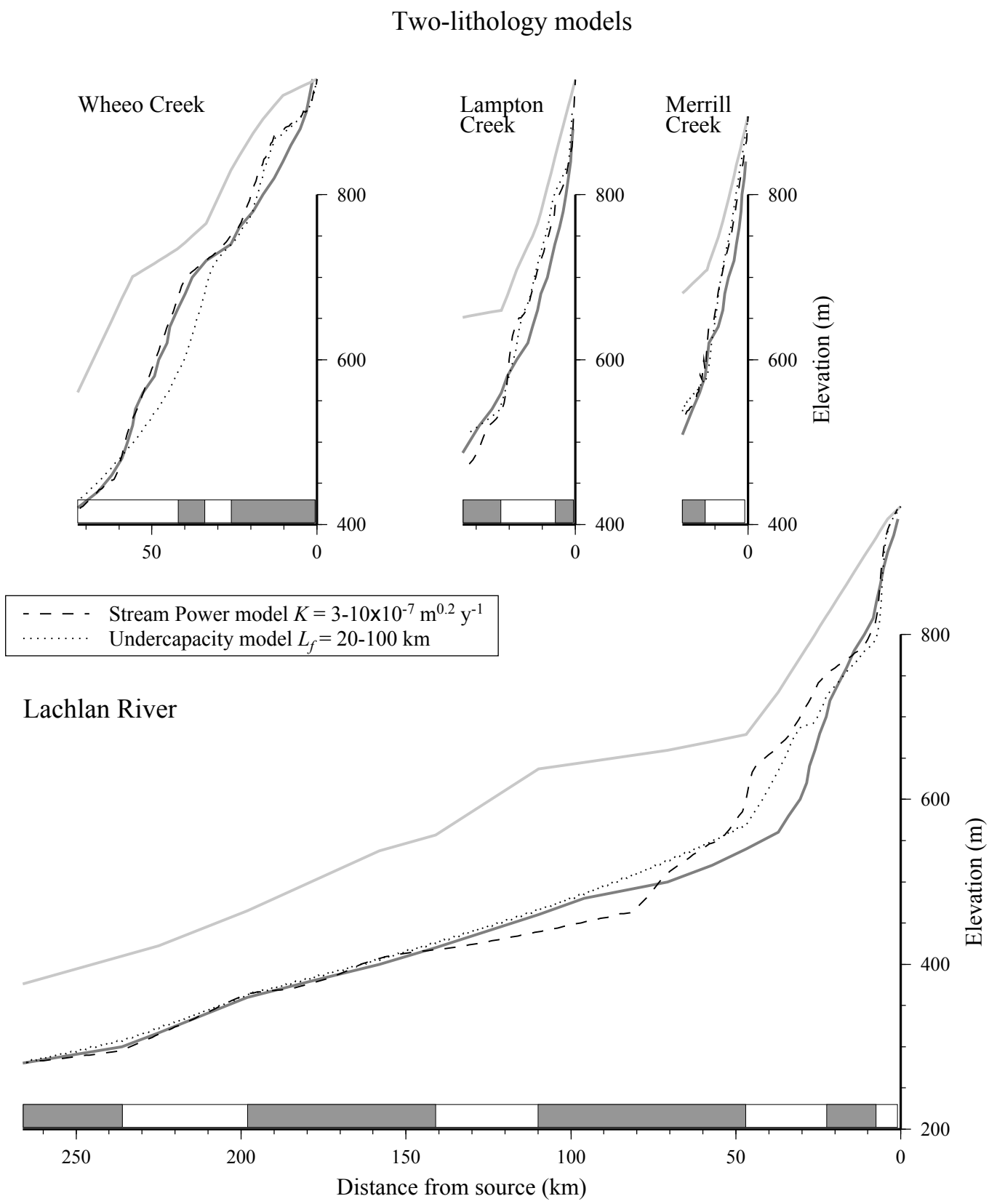

van der Beek and Bishop

Figure 17

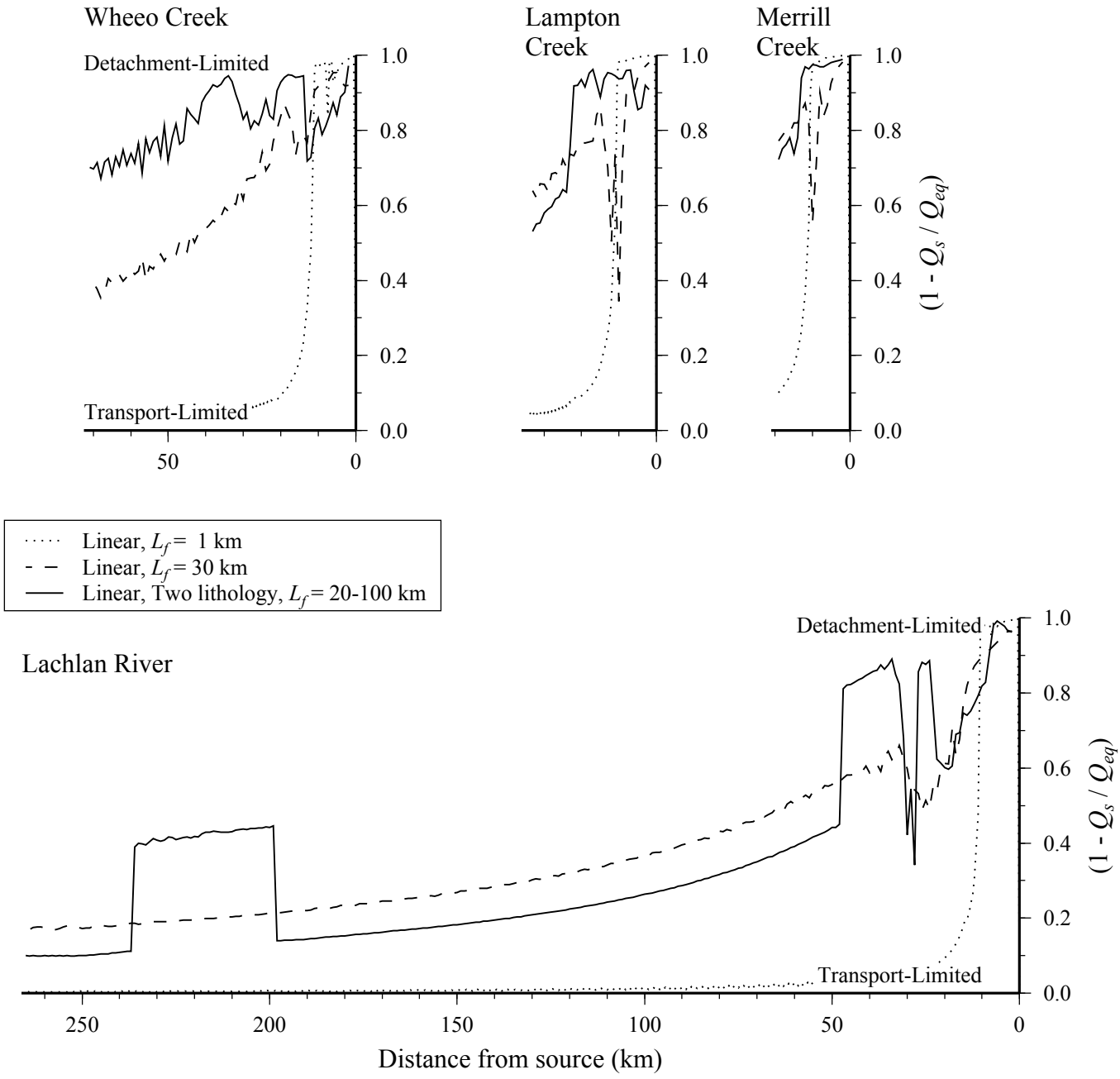

van der Beek and Bishop
Figure 18